CHAPTER 10

Ionic Liquids

10.1 CLASSES AND MODELS OF IONIC LIQUIDS

We have been concerned so far almost exclusively with fluids in which the range of the interparticle forces is of the order of a few atomic radii. This chapter is devoted to systems in which the particles carry an electric charge. Ionic liquids have certain properties that are absent in fluids composed of neutral particles and many of their distinguishing features are associated in some way with the slow decay of the Coulomb potential. Our attention will be focused on three types of system: molten salts, ionic solutions and liquid metals. *Molten salts* are in many respects the simplest class of ionic liquids. We shall consider in detail only the case in which there is a single cation and a single anion species, of which the alkali halides are the best understood examples. Molten salts are characterised by large cohesive energies and high temperatures, and by ionic conductivities of the order of 1 Ω^{-1} cm^{-1}. There exist also certain crystalline salts that have conductivities comparable with those of the molten phase. These are the so-called "fast-ion" conductors, or "solid electrolytes", in which one of the ionic species becomes liquid-like in behaviour above a certain temperature.[1] *Ionic solutions* are liquids consisting of a solvent formed from neutral, polar molecules and a solute that dissociates into positive and negative ions. They vary widely in complexity. In the classic *electrolyte solutions* the cations and anions are of comparable size and absolute charge, whereas macromolecular ionic solutions contain both macroions (charged polymer chains, micelles, charged colloidal particles, etc.) and microscopic counterions. Despite their complexity, some systems of the latter type, including charged colloidal suspensions, can be treated quantitatively by standard methods of liquid-state theory. Finally, *liquid metals* are similar in composition to molten salts, the anion of the salt being replaced by electrons from the valence or conduction bands of the metal. The analogy is a superficial one, however, because the small mass of the electron leads to a pronounced asymmetry between the two charge-carrying species. Whereas the behaviour of the ions can be discussed within the framework of classical statistical mechanics, the electrons form a degenerate Fermi gas for which a quantum-mechanical treatment is required. The presence of "free" electrons is also the origin of the very high electrical conductivies of liquid metals, which are typically three to four orders of magnitude larger than those of molten salts. "Simple" metals are those in which the electronic valence states are well separated in energy from the tightly bound, core states; they include the alkali metals, magnesium, zinc, mercury, gallium and aluminium.

The systems we have listed vary widely in character but they have two important features in common: first, that of overall, macroscopic charge neutrality and, secondly, the presence of mobile charge carriers. The condition of overall charge neutrality imposes a constraint on the relative concentrations of the ions. If the fluid contains $\rho_\nu = N_\nu / V$ ions per unit volume of species ν and if the charge carried by ions of that species is $q_\nu = z_\nu e$, where e is the elementary charge, overall charge neutrality requires that

$$\sum_\nu z_\nu \rho_\nu = 0 \tag{10.1.1}$$

We shall see in the next section that a tendency towards charge neutrality exists even at the local, microscopic level. This effect gives rise in turn to the phenomenon of *screening*. Introduction of an external charge into an ionic fluid causes a rearrangement, or polarisation, of the surrounding charge density of a nature such that the net electrostatic potential due to the external charge and the "polarisation cloud" decays much faster than the bare Coulomb potential. In fact, as we shall show later, the potential decays exponentially. Since it is permissible to regard any ion in the fluid as an "external" charge, it follows that the screening mechanism determines the long-range behaviour of the ionic distribution functions. Screening also requires that the distribution functions satisfy a number of important sum rules. In ionic liquids of high density, such as molten salts, there is a competition between packing effects and screening; this leads to a *charge ordering* of the ions, which manifests itself as an alternation in sign of the charge carried by successive coordination shells around a central ion.

The presence of mobile charge carriers plays an important role in determining the dynamical properties of ionic liquids. It leads most obviously to new kinds of transport, of which electrical conduction is the most familiar example. In addition, the interplay between Maxwell's equations and the equations of hydrodynamics causes the long-wavelength charge fluctuations to relax in a manner qualitatively different from that of concentration fluctuations in mixtures of uncharged particles. Under conditions achievable, in particular, in molten salts, fluctuations in charge may give rise to propagating, high-frequency, collective modes. These excitations are similar in character to the optic modes of ionic crystals and are also closely related to the charge oscillations found in plasmas.

Theories of ionic liquids rely heavily on the use of simple hamiltonian models that retain only the essential features of the ionic interactions. One simplifying approximation commonly made is to ignore the polarisability of the ions and represent the interactions by a *rigid-ion model*. The total potential energy is then assumed to be pairwise-additive and written as the sum of short-range (S) and coulombic (C) terms in the form

$$V_N(\mathbf{r}^N) = V_N^{\mathrm{S}}(\mathbf{r}^N) + V_N^{\mathrm{C}}(\mathbf{r}^N) = V_N^{\mathrm{S}}(\mathbf{r}^N) + \sum_{i=1}^{N} \sum_{j>i}^{N} \frac{z_i z_j e^2}{\varepsilon |\mathbf{r}_j - \mathbf{r}_i|} \tag{10.1.2}$$

where N is the total number of ions and ε is the dielectric constant of the medium in which the ions are immersed. It is often convenient to replace the Coulomb term in (10.1.2) by a sum in reciprocal space. Let $\rho_{\mathbf{k}}^Z$ be a Fourier component of the microscopic charge density,

given by

$$\rho_{\mathbf{k}}^{Z} = \sum_{\nu} z_{\nu} \rho_{\mathbf{k}}^{\nu} \tag{10.1.3}$$

where $\rho_{\mathbf{k}}^{\nu}$ is a Fourier component of the microscopic number density of species ν. Then the total Coulomb energy of a periodic system of volume V is

$$V_N^{\mathrm{C}}(\mathbf{r}^N) = \frac{1}{2V} \sum_{\mathbf{k}} \hat{v}(k) \left(\rho_{\mathbf{k}}^{Z} \rho_{-\mathbf{k}}^{Z} - \sum_{i=1}^{N} z_i^2 \right) \tag{10.1.4}$$

where the sum on $\mathbf{k}$ runs over wavevectors compatible with the assumed periodic boundary conditions and the (negative) second term inside brackets cancels the infinite self-energy of the ions. The function $\hat{v}(k)$ is the Fourier transform of the Coulomb potential between two elementary charges, i.e.

$$\hat{v}(k) = 4\pi e^2 / k^2 \tag{10.1.5}$$

The same expression was used earlier in the derivation of the Debye–Hückel result (4.6.26); the k^{-2} singularity in the limit $k \to 0$ is an important characteristic of Coulomb systems. In the thermodynamic limit the sum over wavevectors in (10.1.4) becomes an integral over $\mathbf{k}$ divided by $(2\pi)^3$; the equivalence of the two expressions for V_N^{C} in (10.1.2) and (10.1.4) is then an immediate consequence of elementary properties of the Fourier transform.

If electrical neutrality is to be achieved, an ionic fluid must contain at least two species of opposite charge. The simplest representation of such a system is obtained by replacing one of the species by a uniformly smeared-out, structureless background, the total charge of which must cancel that of the discrete ions. When the discrete ions are identical point charges, the resulting model (already discussed in Section 4.6) is called the *one-component plasma* or OCP.[2] The total potential energy of an OCP in which the ions carry a charge ze is given by the sum over $\mathbf{k}$ in (10.1.4), with $\rho_{\mathbf{k}}^{Z} = z\rho_{\mathbf{k}}$, except that the presence of the neutralising background means that the term for $\mathbf{k} = 0$ must be omitted. The OCP has certain unphysical features. For example, mass and charge fluctuations are proportional to each other and the system therefore has zero resistivity, because conservation of total momentum is equivalent to conservation of the microscopic electric current. Nevertheless, as the prototypical ionic fluid, the OCP plays a conceptual role similar to that filled by the hard-sphere model in the theory of simple, insulating liquids. It provides, in particular, a useful starting point for the study of liquid metals, where the mobile species corresponds to the metal ions and the background represents the conduction electrons.

To illustrate the usefulness of the OCP in the qualitative discussion of the properties of ionic liquids we return briefly to the question of the high-frequency, charge-fluctuation modes mentioned earlier. The characteristic frequency of the longitudinal mode is the plasma frequency, ω_{p}. In the case of the OCP an expression for ω_{p} can be obtained by a simple argument based on a δ-function representation of the dynamic structure factor. Use of such a model is justified by the fact that conservation of momentum of the ions means that there is no damping of charge fluctuations in the long-wavelength limit. We therefore assume that $S(k, \omega)$ consists of a pair of δ-functions located at frequencies $\pm\omega_k$,

and identify the plasma frequency as $\omega_p = \lim_{k\to 0}\omega_k$. If the spectrum is to satisfy the sum rules (7.4.23) and (7.4.30), ω_k must be such that

$$\omega_k^2 = \frac{\omega_0^2}{S(k)} = \frac{k_B T}{mS(k)}k^2 \tag{10.1.6}$$

The long-wavelength limit of $S(k)$ can be estimated within the random-phase approximation of Section 5.5. If we choose the ideal gas as reference system and make the substitution $\hat{c}(k) = -\beta z^2 \hat{v}(k)$, (5.5.25) becomes

$$S(k) = \frac{1}{1+\beta\rho z^2\hat{v}(k)} = \frac{1}{1+4\pi\beta\rho z^2 e^2/k^2} \sim \frac{k^2}{k_D^2}, \quad k \to 0 \tag{10.1.7}$$

where k_D is the Debye wavenumber defined by (4.6.23); as we shall see later, (10.1.7) is exact for the OCP. If we now substitute for $S(k)$ in (10.1.6), we find that

$$\omega_p^2 = \lim_{k\to 0}\omega_k^2 = \frac{4\pi\rho z^2 e^2}{m} \tag{10.1.8}$$

The frequency of the propagating mode therefore remains non-zero even in the long-wavelength limit; this is a characteristic feature of an optic-type excitation. The fact that ω_p is non-zero is a direct consequence of the k^{-2} singularity in $\hat{v}(k)$, since it is this singularity that determines the small-k behaviour of $S(k)$. Note also that the plasma frequency is independent of temperature.

If the fluid is genuinely two-component in character, a short-range repulsion is essential if the system is to be stable against the collapse of oppositely charged pairs. Within a model, stability is most easily achieved by imposing a hard-sphere repulsion between ions, a choice of interaction that defines the *primitive model* of electrolytes and molten salts. The primitive model has been widely adopted in studies of the osmotic properties of ionic solutions, the solvent being replaced by a continuum of dielectric constant ε that acts to reduce the Coulomb interaction between ions; the *restricted* version of the model is one in which all ions have the same diameter, d, and the same absolute valency, z.

The restricted primitive model with $\varepsilon = 1$ provides the simplest example of a rigid-ion model of a molten salt. Alternatively, the short-range interactions in the salt can be modelled by soft-core repulsions characterised by a single length parameter σ. For example, the short-range contribution to the pair potential can be written as

$$v_{\nu\mu}^S(r) = \frac{z^2e^2}{n\sigma}\left(\frac{\sigma}{r}\right)^n \tag{10.1.9}$$

for all pairs ν, μ; the parameter σ is the separation at which the cation–anion potential has its minimum value. Equation (10.1.9), together with the coulombic term, defines what we shall call the "simple molten salt". This provides a fair representation of the ionic interactions in the molten alkali halides, particularly of salts in which the positive and negative ions are of approximately equal size. The values of n appropriate to the alkali

halides are in the range $n = 8$ to 10; in the limit $n \to \infty$, the simple molten salt reduces to the restricted primitive model. If the two ionic species have equal masses, the hamiltonian of the system is fully symmetric under charge conjugation, meaning that cations and anions play identical roles.

The examples given in later sections of this chapter draw heavily on calculations for the restricted primitive model and the simple molten salt, but a number of more realistic models appropriate to molten salts have also been extensively studied both theoretically and by simulation. The best known of these are the rigid-ion potentials derived for salts of the alkali-halide family[3] in which the short-range interaction between a given ion pair is written as the sum of an exponential repulsion and attractive terms arising from dipole–dipole and dipole–quadrupole dispersion forces. If the ions are highly polarisable, however, as is often the case for the anion, the effect of induction forces cannot be ignored. A variety of schemes have therefore been devised that allow the incorporation of ionic polarisation into molecular-dynamics simulations of molten salts. Much of the early work on polarisable systems was based on the "shell model" of lattice dynamics, in which the total charge of the ion is divided between a core and a massless shell. The shell is bound to the core by a harmonic potential and polarisation of the ion corresponds to a bodily shift of the shell relative to the core; the shells, being of zero mass, are assumed to adjust themselves instantaneously in such a way as to minimise the total potential energy. Some interesting results have been obtained in this way, but the model has a number of unsatisfactory features. For example, the parameters characterising a particular ion species are not transferable from one salt to another. A different approach has subsequently been developed[4] in which the dipole moments are treated as additional degrees of freedom within an "extended lagrangian" scheme; this method resembles closely one devised earlier for the treatment of many-body polarisation effects in polar fluids.[5]

10.2 SCREENING AND CHARGE ORDERING

The microscopic structure of an n-component ionic fluid can be discussed in terms of $\frac{1}{2}n(n+1)$ partial structure factors $S_{\nu\mu}(k)$ with $\nu,\ \mu = 1$ to n, but it is certain linear combinations of these functions that are of most physical relevance. If

$$\rho_{\mathbf{k}}^{N} = \sum_{\nu} \rho_{\mathbf{k}}^{\nu} \tag{10.2.1}$$

is a Fourier component of the microscopic number density, and if the components of the charge density are defined as in (10.1.3), fluctuations in the densities are described by three static structure factors of the form

$$S_{NN}(k) = \frac{1}{N}\langle \rho_{\mathbf{k}}^{N} \rho_{-\mathbf{k}}^{N} \rangle = \sum_{\nu}\sum_{\mu} S_{\nu\mu}(k) \tag{10.2.2a}$$

$$S_{NZ}(k) = \frac{1}{N}\langle \rho_{\mathbf{k}}^{N} \rho_{-\mathbf{k}}^{Z} \rangle = \sum_{\nu}\sum_{\mu} z_{\mu} S_{\nu\mu}(k) \tag{10.2.2b}$$

$$S_{ZZ}(k) = \frac{1}{N}\langle \rho^Z_{\mathbf{k}} \rho^Z_{-\mathbf{k}} \rangle = \sum_\nu \sum_\mu z_\nu z_\mu S_{\nu\mu}(k) \tag{10.2.2c}$$

Of these three functions, the number–number structure factor $S_{NN}(k)$ is the closest in significance to the single structure factor of a one-component fluid.

Let $\delta\phi_\mu(\mathbf{r})$ be a weak, external potential that couples to the microscopic number density of species μ. We saw in Section 3.6 that the change induced in a Fourier component of the single-particle density of species ν is

$$\delta\hat{\rho}^{(1)}_\nu(\mathbf{k}) = \chi_{\nu\mu}(k)\delta\hat{\phi}_\mu(\mathbf{k}) \tag{10.2.3}$$

where the static response function $\chi_{\nu\mu}(k)$ is related to the corresponding partial structure factor by

$$\chi_{\nu\mu}(k) = -\beta\rho S_{\nu\mu}(k) \tag{10.2.4}$$

The problem of greatest interest here concerns the response of the fluid to a weak field produced by an external charge density with Fourier components $e\delta\hat{\rho}^{\text{ext}}(\mathbf{k})$; to simplify the discussion we consider a system of rigid ions *in vacuo* ($\varepsilon = 1$). The electric potential due to the external charge density is obtained from the **k**-space version of Poisson's equation, i.e.

$$\delta\hat{\phi}^{\text{ext}}(\mathbf{k}) = \frac{4\pi e}{k^2}\delta\hat{\rho}^{\text{ext}}(\mathbf{k}) \tag{10.2.5}$$

The electric potential couples directly to the microscopic charge density of the fluid, giving rise to a mean induced charge density $\delta\hat{\rho}_Z(\mathbf{k})$. The latter is proportional to $e\delta\hat{\phi}^{\text{ext}}(\mathbf{k})$, the constant of proportionality being, by definition, the charge-density response function, $\chi_{ZZ}(k)$. Thus

$$\delta\hat{\rho}_Z(\mathbf{k}) = \sum_\nu z_\nu \delta\hat{\rho}^{(1)}_\nu(\mathbf{k}) = \chi_{ZZ}(k)e\delta\hat{\phi}^{\text{ext}}(\mathbf{k}) \tag{10.2.6}$$

If we put $\delta\hat{\phi}_\mu(\mathbf{k}) = z_\mu e\delta\hat{\phi}^{\text{ext}}(\mathbf{k})$ in (10.2.3) and then substitute for $\delta\hat{\rho}^{(1)}_\nu(\mathbf{k})$ in (10.2.6), we find that the response function can be identified as

$$\chi_{ZZ}(k) = \sum_\nu \sum_\mu z_\nu z_\mu \chi_{\nu\mu}(k) \tag{10.2.7}$$

and combination of (10.2.2c), (10.2.4) and (10.2.7) leads to the charge-response version of the fluctuation–dissipation theorem:

$$\chi_{ZZ}(k) = -\beta\rho S_{ZZ}(k) \tag{10.2.8}$$

The electrostrictive behaviour of the fluid, i.e. the number-density response to an external electric potential, is characterised by a cross response function $\chi_{NZ}(k)$ through an expression analogous to (10.2.6):

$$\delta\hat{\rho}_N(\mathbf{k}) = \sum_\nu \delta\hat{\rho}^{(1)}_\nu(\mathbf{k}) = \chi_{NZ}(k)e\delta\hat{\phi}^{\text{ext}}(\mathbf{k}) \tag{10.2.9}$$

The charge response to the external potential can equally well be described in terms of a longitudinal dielectric function $\varepsilon(k)$; this is simply a k-dependent generalisation of the macroscopic dielectric constant of elementary electrostatics. If **E** is the electric field and **D** is the electric displacement, $\varepsilon(k)$ is given by

$$\frac{1}{\varepsilon(k)} = \frac{\mathbf{k}\cdot\widehat{\mathbf{E}}(k)}{\mathbf{k}\cdot\widehat{\mathbf{D}}(k)} = 1 + \frac{\delta\hat{\rho}_Z(\mathbf{k})}{\delta\hat{\rho}^{\text{ext}}(\mathbf{k})} \tag{10.2.10}$$

where Maxwell's equations have been used to relate **E** and **D**, respectively, to the total and external charge densities. Equations (10.2.5), (10.2.6) and (10.2.10) can now be combined to yield the fundamental relation between the dielectric and charge-response functions:

$$\frac{1}{\varepsilon(k)} = 1 + \frac{4\pi e^2}{k^2}\chi_{ZZ}(k) \tag{10.2.11}$$

The definition (10.2.2c) shows that $S_{ZZ}(k)$ can never be negative. Equations (10.2.8) and (10.2.11) therefore imply that $1/\varepsilon(k) \leqslant 1$ for all k.

It is known experimentally that an external charge distribution is completely screened by a conducting fluid. In other words, the total charge density vanishes in the long-wavelength limit, or

$$\lim_{\mathbf{k}\to 0}\left[\delta\hat{\rho}^{\text{ext}}(\mathbf{k}) + \delta\hat{\rho}_Z(\mathbf{k})\right] = 0 \tag{10.2.12}$$

If this result is to be consistent with (10.2.10), it follows that

$$\lim_{k\to 0}\varepsilon(k) = \infty \tag{10.2.13}$$

In combination with (10.2.8) and (10.2.11), the assumption of *perfect screening* contained in (10.2.13) implies that the charge structure factor at long wavelengths behaves as

$$\lim_{k\to 0}\frac{k_{\text{D}}^2}{k^2}S_{ZZ}(k) = \sum_\nu x_\nu z_\nu^2 \tag{10.2.14}$$

where $x_\nu = \rho_\nu/\rho$ and k_{D}, the Debye wavenumber, is given by a generalisation of (4.6.23):

$$k_{\text{D}}^2 = \frac{4\pi\beta\rho e^2}{\varepsilon}\sum_\nu x_\nu z_\nu^2 \tag{10.2.15}$$

The quantity $\Lambda_{\text{D}} = 1/k_{\text{D}}$ is the Debye screening length, familiar from ionic-solution theory; in a dilute electrolyte it is the distance beyond which the electric potential due to an ion is completely screened by the local, induced charge distribution. From comparison of (10.2.14) with the compressibility equation (3.6.11) we see that large-scale (long-wavelength) charge fluctuations are strongly inhibited in comparison with the number-density fluctuations of a neutral fluid. It has been proved rigorously[6] that the fluctuation in the total charge Q_V contained in a volume V, i.e. $(\langle Q_V^2\rangle - \langle Q_V\rangle^2)$, is proportional only

to the surface area bounding the volume. By contrast, (2.4.23) shows that the fluctuation in the number of particles within V is proportional to V itself.

Equation (10.2.14) leads directly to two important relations between the partial pair distribution functions of an ionic fluid, known as the Stillinger–Lovett sum rules.[7] We see from (3.6.15) and (10.2.2c) that the charge structure factor is related to the partial pair correlation functions $h_{\nu\mu}(r)$ by

$$S_{ZZ}(k) = \sum_{\nu}\sum_{\mu} z_\nu z_\mu \left(x_\nu \delta_{\nu\mu} + 4\pi\rho x_\nu x_\mu \int_0^\infty \frac{\sin kr}{kr} h_{\nu\mu}(r) r^2 \, \mathrm{d}r \right) \tag{10.2.16}$$

If the functions $h_{\nu\mu}(r)$ decay sufficiently rapidly at large r, the Fourier integrals in (10.2.16) may be expanded to order k^2. The two sum rules are then obtained by equating terms of zeroth and second order in k in (10.2.14) and (10.2.16) and exploiting the condition of overall charge neutrality expressed by (10.1.1). The results derived in this way are

$$\begin{aligned} \rho \sum_{\nu} x_\nu z_\nu \sum_{\mu} \int x_\mu z_\mu g_{\nu\mu}(r) \, \mathrm{d}\mathbf{r} &= -\sum_{\nu} x_\nu z_\nu^2 \\ \rho \sum_{\nu} x_\nu z_\nu \sum_{\mu} \int x_\mu z_\mu g_{\nu\mu}(r) r^2 \, \mathrm{d}\mathbf{r} &= -6\Lambda_{\mathrm{D}}^2 \sum_{\nu} x_\nu z_\nu^2 \end{aligned} \tag{10.2.17}$$

The assumption concerning the large-r behaviour of the correlation functions is equivalent to a "clustering" hypothesis for the particle densities. An n-particle density $\rho^{(n)}(\mathbf{r}^n)$ is said to have a clustering property if, for all $m < n$, it reduces to the product $\rho^{(m)}(\mathbf{r}^m)\rho^{(n-m)}(\mathbf{r}^{(n-m)})$ faster than a prescribed inverse power of the distance between the centres of mass of the clusters $(\mathbf{r}_1, \ldots, \mathbf{r}_m)$ and $(\mathbf{r}_{m+1}, \ldots, \mathbf{r}_n)$ as the clusters become infinitely separated. If the clustering hypothesis is used, the Stillinger–Lovett sum rules can be derived from the YBG hierarchy of Section 4.2 without making any assumption about the small-k behaviour of $S_{ZZ}(k)$. The derivation is therefore not dependent on the perfect-screening condition (10.2.13); perfect screening appears instead as a consequence of the sum rules.

The first of the Stillinger–Lovett rules is just a linear combination of local electroneutrality conditions of the form

$$\rho \sum_{\mu} \int x_\mu z_\mu g_{\nu\mu}(r) \, \mathrm{d}\mathbf{r} = -z_\nu \tag{10.2.18}$$

The physical meaning of (10.2.18) is that the total charge around a given ion must exactly cancel the charge of the ion. This is the first of a series of sum rules satisfied by the multipole moments of the charge distribution in the vicinity of a given number of fixed ions.[8] The sum rules can again be derived from the YBG hierarchy if appropriate clustering assumptions are made. In particular, if correlations are assumed to decay exponentially, it can be shown that the charge distribution around any number of fixed ions has no multipole moment of any order. The local electroneutrality condition may be re-expressed in

terms of the long-wavelength limits of the partial structure factors. In the case of a two-component system, (10.2.18) becomes $z_1^2 S_{11}(0) = -z_1 z_2 S_{12}(0) = z_2^2 S_{22}(0)$ or, because the fluid is electrically neutral overall:

$$x_2^2 S_{11}(0) = x_1 x_2 S_{12}(0) = x_1^2 S_{22}(0) \tag{10.2.19}$$

No such property holds for the partial structure factors of a mixture of neutral fluids.

The $k \to 0$ limits of the partial structure factors of a binary ionic fluid are related to the isothermal compressibility via the Kirkwood–Buff formula (3.6.17). The conditions imposed by charge neutrality mean, however, that direct substitution of (10.2.19) in (3.6.17) leads to an indeterminate result. To avoid this problem we invert the system of linear equations represented by (10.2.2) and rewrite (3.6.17) in terms of $S_{NN}(k)$, $S_{NZ}(k)$ and $S_{ZZ}(k)$ in the form

$$\rho k_{\mathrm{B}} T \chi_T = \lim_{k \to 0} \frac{S_{NN}(k) S_{ZZ}(k) - S_{NZ}^2(k)}{S_{ZZ}(k)} \tag{10.2.20}$$

The small-k limits of the three structure factors in (10.2.20) can be deduced from the asymptotic behaviour of the partial direct correlation functions $c_{\nu\mu}(r)$. At large r we may expect these functions to decay as $c_{\nu\mu}(r) \sim -\beta z_\nu z_\mu e^2/r$. It is therefore natural to separate $c_{\nu\mu}(r)$ into short-range and coulombic parts; in $\mathbf{k}$-space $\hat{c}_{\nu\mu}(k)$ becomes

$$\hat{c}_{\nu\mu}(k) = \hat{c}_{\nu\mu}^{\mathrm{S}}(k) - \frac{4\pi\beta z_\nu z_\mu e^2}{k^2} \tag{10.2.21}$$

where $\hat{c}_{\nu\mu}^{\mathrm{S}}(k)$ is a regular function in the limit $k \to 0$. Substitution of (10.2.21) in the Ornstein–Zernike relation (3.6.12) leads, after some straightforward algebra and use of (10.1.1) and (10.2.2), to the required results: at small k, $S_{NN}(k) \sim k^0$, $S_{NZ}(k) \sim k^2$ and $S_{ZZ}(k) \sim k^2$; the last result agrees with (10.2.14). Thus (10.2.20) reduces to the simpler expression

$$\rho k_{\mathrm{B}} T \chi_T = \lim_{k \to 0} S_{NN}(k) \tag{10.2.22}$$

while (3.6.16) becomes

$$\frac{1}{\rho k_{\mathrm{B}} T \chi_T} = 1 - \rho \lim_{k \to 0} \sum_\nu \sum_\mu x_\nu x_\mu \hat{c}_{\nu\mu}^{\mathrm{S}}(k) \tag{10.2.23}$$

Because fluctuations in concentration correspond to fluctuations in charge density, and because such fluctuations are suppressed at long wavelengths, all reference to the two-component nature of the fluid has vanished from (10.2.22), which therefore resembles the corresponding result for a one-component system of uncharged particles.

The coefficients of the terms of order k^4 in the small-k expansions of $S_{ZZ}(k)$ and $S_{NZ}(k)$ and those of order k^2 in the expansion of $S_{NN}(k)$ can be determined by macroscopic arguments based on linearised hydrodynamics or thermodynamic fluctuation theory. We give here the corresponding calculation for the OCP, where the problem is simplified by the fact

that fluctuations in particle number are equivalent to fluctuations in charge. In the absence of any flow the force per unit volume due to the electric field must exactly balance the force due to the pressure gradient. Thus

$$ze\rho\mathbf{E}(\mathbf{r}) = \nabla P(\mathbf{r}) \tag{10.2.24}$$

where $ze\rho$ is the mean charge density of the mobile ions and the field $\mathbf{E}(\mathbf{r})$ is related to the sum of external and induced charge densities by Poisson's equation:

$$\nabla \cdot \mathbf{E}(\mathbf{r}) = 4\pi e\left[\delta\rho^{\text{ext}}(\mathbf{r}) + \delta\rho_Z(\mathbf{r})\right] \tag{10.2.25}$$

If the system is in local thermodynamic equilibrium, the pressure change in an isothermal process is

$$\delta P(\mathbf{r}) \equiv P(\mathbf{r}) - P = \left(\frac{\partial P}{\partial \rho}\right)_T \delta\rho(\mathbf{r}) = \frac{1}{z\rho\chi_T}\,\delta\rho_Z(\mathbf{r}) \tag{10.2.26}$$

Equations (10.2.24) to (10.2.26) may now be combined to give a differential equation for $\delta\rho_Z(\mathbf{r})$ of the form

$$\frac{1}{k_s^2}\nabla^2\delta\rho_Z(\mathbf{r}) - \delta\rho_Z(\mathbf{r}) = \delta\rho^{\text{ext}}(\mathbf{r}) \tag{10.2.27}$$

where

$$k_s^2 = 4\pi z^2 e^2 \rho^2 \chi_T = k_D^2 \frac{\chi_T}{\chi_T^{\text{id}}} \tag{10.2.28}$$

The solution to (10.2.27), obtained by taking Fourier transforms, is

$$\delta\hat{\rho}_Z(\mathbf{k}) = -\frac{\delta\hat{\rho}^{\text{ext}}(\mathbf{k})}{1 + k^2/k_s^2} \tag{10.2.29}$$

Comparison of (10.2.29) with (10.2.10) shows that the long-wavelength limit of $\varepsilon(k)$ is

$$\lim_{k\to 0} \varepsilon(k) = 1 + k_s^2/k^2 \tag{10.2.30}$$

which clearly satisfies the perfect-screening condition (10.2.13). The corresponding long-wavelength expression for $S_{ZZ}(k)$ $(= z^2 S(k))$, derived from (10.2.8) and (10.2.11), is

$$\lim_{k\to 0} S_{ZZ}(k) = \frac{z^2 k^2/k_D^2}{1 + k^2/k_s^2} \tag{10.2.31}$$

in agreement with (10.1.7). Equations (10.2.30) and (10.2.31) also apply to mixtures of oppositely charged ions with $z_1 = -z_2 = z$, except that k_s is differently defined.[9]

The Fourier components of the total electrostatic potential $\delta\phi(\mathbf{r})$ are related to the components of the total charge density by the analogue of (10.2.5). In the long-wavelength

limit it follows from (10.2.10) and (10.2.30) that

$$\delta\hat{\phi}(\mathbf{k}) = \frac{4\pi e}{k^2}\left[\delta\hat{\rho}^{\text{ext}}(\mathbf{k}) + \delta\hat{\rho}_Z(\mathbf{k})\right]$$
$$= \frac{4\pi e}{k^2\varepsilon(k)}\delta\hat{\rho}^{\text{ext}}(\mathbf{k}) = \frac{4\pi e}{k^2 + k_s^2}\delta\hat{\rho}^{\text{ext}}(\mathbf{k}) \tag{10.2.32}$$

If an ion of species ν in the fluid is regarded as an "external" charge placed at the origin, the "external" charge density is $e\delta\rho^{\text{ext}}(\mathbf{r}) = z_\nu e\delta(\mathbf{r})$, and (10.2.32) shows that the effective potential due to the ion decays as

$$\phi_\nu(r) = \frac{z_\nu e}{r}\exp(-k_s r) \tag{10.2.33}$$

The quantity $\phi_\nu(r)$ $(= \delta\phi(r))$ is the potential of mean force for ions of species ν. In the case of the OCP, k_s is given by (10.2.28); this becomes equal to the Debye wavenumber in the weak-coupling limit ($\rho \to 0$ or $T \to \infty$), where χ_T may be replaced by its ideal-gas value, $\chi_T^{\text{id}} = \beta\rho$. With these simplifications, (10.2.33) reduces to the Debye–Hückel result (4.6.25). In the strong-coupling regime the compressibility of the OCP becomes negative, k_s takes on imaginary values, and the potential of mean force develops the oscillations characteristic of systems with short-range order.

Oscillations of the charge density around a given ion are also a feature of two-component ionic fluids, where they arise as a result of competition between hard-core packing and local charge neutrality. In the case of the restricted primitive model a simple argument[7(a)] based on the sum rules (10.2.17) shows that the radial charge distribution function $[g_{11}(r) - g_{12}(r)]$ (or $[g_{22}(r) - g_{12}(r)]$) must change sign as a function of r if $k_D d \geqslant \sqrt{6}$. Charge ordering of this type is a very strong effect in molten salts and oscillations in the charge density around a central ion extend over many ionic radii. Computer simulations of a variety of monovalent salts show that the pair distribution functions for ions of like sign, $g_{11}(r)$ and $g_{22}(r)$, are very similar in form and that the oscillations in these two functions are almost exactly out of phase with those in the much more sharply peaked, cation–anion distribution function $g_{12}(r)$. Thus the radial charge distribution functions around either a cation or anion are essentially the same and strongly oscillatory. The similarity between $g_{11}(r)$ and $g_{22}(r)$ gives support to the use of the simple molten salt defined by (10.1.9) as a model of the alkali halides. Some molecular-dynamics results for such a model (with $n = 9$) are shown in Figure 10.1. The regular alternation of concentric shells of oppositely charged ions is clearly visible in the pair distribution functions plotted in part (a) of the figure. In **k**-space the effects of charge ordering reflect themselves in the very sharp main peak in the charge–charge structure factor $S_{ZZ}(k)$ (the Fourier transform of $[g_{11}(r) + g_{22}(r) - 2g_{12}(r)]$), shown in part (b); by contrast, $S_{NN}(k)$ (the transform of $[g_{11}(r) + g_{22}(r) + 2g_{12}(r)]$) is a relatively structureless function. The symmetry of the model means that charge and number fluctuations are completely decoupled; thus $S_{NZ}(k)$ is zero at all k. In the general case, the fluctuations are strictly independent only in the long-wavelength limit, since $S_{NZ}(k) \sim k^2$ as $k \to 0$.

The main structural features exhibited by the simple molten salt are also seen in computer simulations of more realistic rigid-ion models of the alkali halides. The results are

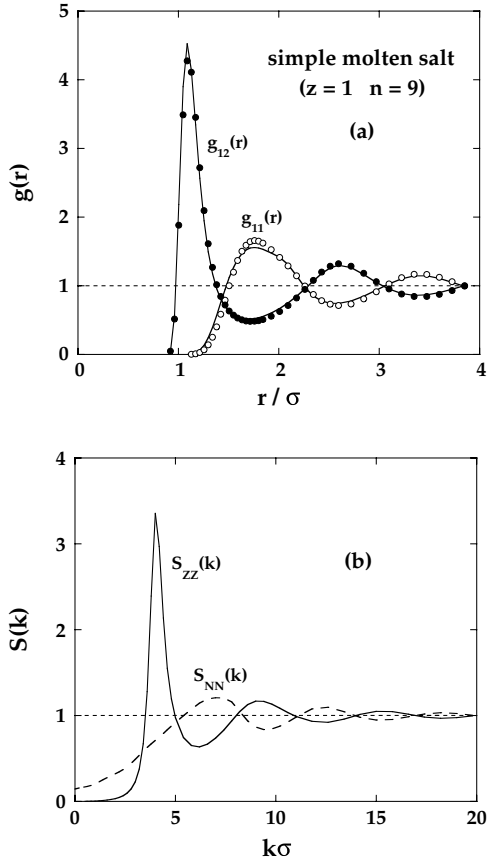

FIG. 10.1. Charge ordering in the simple molten salt[10] in a thermodynamic state corresponding roughly to that of molten sodium chloride at $T \approx 1270$ K. (a) Distribution functions for cation–anion and cation–cation (or anion–anion) pairs. The points show the results of molecular-dynamics calculations and the curves are calculated from the HNC approximation (see Section 10.3). (b) Molecular-dynamics results for the static charge–charge and number–number structure factors.

consistent with those obtained by neutron-scattering experiments, which rely on the use of isotopic substitution to separate the contributions of the partial structure factors $S_{\nu\mu}(k)$ to the measured cross-section. Similar experiments have been carried out for the alkaline-earth halides and are again in good general agreement with those obtained in simulations based on rigid-ion models. Because the absolute charges of the two ionic species are now different, the marked similarity seen in the alkali halides between $g_{11}(r)$ and $g_{22}(r)$ is lost.

10.3 INTEGRAL-EQUATION THEORIES

The techniques introduced in Chapters 3 to 5 provide a number of possible routes to the calculation of thermodynamic and structural properties of simple ionic liquids. Versions of

the optimised cluster theory of Section 5.5 and other, closely related methods have proved particularly successful in describing the thermodynamic behaviour of dilute systems. In this section, however, we focus on the integral-equation approach, in which the emphasis is placed on the calculation of the pair distribution functions. Much of the published work in this field is concerned with the alkali halides, either in the molten phase or in solution, though there has also been considerable interest in the properties of 2 : 1 and 2 : 2 electrolyte solutions, the structure of which is characterised by a high degree of ionic association. The physical conditions are, of course, very different in the molten-salt and electrolyte regimes. If we adopt the primitive model of Section 10.1, the thermodynamic state is conveniently characterised by the reduced density $\rho^* = Nd^3/V$, where N is the total number of ions and $d = \frac{1}{2}(d_{11} + d_{22})$ is the mean ionic diameter, and a reduced Coulomb coupling parameter, or inverse temperature, defined as

$$\beta^* = \frac{|z_1 z_2| e^2}{\varepsilon k_B T d} \tag{10.3.1}$$

Near the melting point of an alkali halide, $\rho^* \approx 0.4$ and $\beta^* \approx 65$, while for a 1 M aqueous solution of the same salt at room temperature, $\rho^* \approx 0.01$ and $\beta^* \approx 3$. We must therefore expect the nature of the interionic correlations to be very different in the two cases. The liquid–vapour phase diagram of a molten alkali halide is qualitatively similar to that, say, of a rare gas, but the reduced critical densities of the salts are only about one-third of those of typical insulating liquids.

The value of different theoretical approaches can be illustrated by limiting attention initially to systems of charged hard spheres and, in particular, to the restricted primitive model, with $z_1 = -z_2 = 1$. A convenient starting point for the discussion is the mean spherical approximation (MSA) introduced in Section 4.5, since in this case the MSA has a completely analytic solution.[11] The MSA for equisized hard spheres of diameter d is

$$g_{\nu\mu} = 0, \quad r < d; \qquad c_{\nu\mu}(r) = -\frac{\beta z_\nu z_\mu e^2}{\varepsilon r}, \quad r > d \tag{10.3.2}$$

which must be used in conjunction with the Ornstein–Zernike relation for equimolar binary mixtures; this is obtained as a special case of (3.6.12), with $x_1 = x_2 = \frac{1}{2}$. The symmetry of the restricted primitive model allows the Ornstein–Zernike relation to be rewritten as two independent equations for the linear combinations

$$h_S(r) = \tfrac{1}{2}\big[h_{11}(r) + h_{12}(r)\big], \qquad h_D(r) = h_{11}(r) - h_{12}(r) \tag{10.3.3}$$

and the corresponding direct correlation functions $c_S(r)$ and $c_D(r)$; $h_S(r)$ is a number-density correlation function and $h_D(r)$ describes the correlation in charge density. When written in terms of the new functions the MSA becomes

$$h_S(r) = -1, \quad r < d; \qquad c_S(r) = 0, \quad r > d \tag{10.3.4a}$$

$$h_D(r) = 0, \quad r < d; \qquad c_D(r) = -\frac{2\beta e^2}{\varepsilon r}, \quad r > d \tag{10.3.4b}$$

The closure relation (10.3.4a) is just the Percus–Yevick approximation for hard spheres, for which the solution is known (see Section 4.4). The solution to (10.3.4b) and the associated Ornstein–Zernike relation between $h_D(r)$ and $c_D(r)$ can also be obtained in closed form by incorporating the sum rules (10.2.17) into generalised versions of the methods used to solve the PY equation for hard spheres. The result for $c_D(r)$ inside the hard core is

$$c_D(r) = -\frac{2\beta e^2}{\varepsilon d}(2 - Br/d)B \tag{10.3.5}$$

with $B = [\xi + 1 - (1 + 2\xi)^{1/2}]/\xi$, where $\xi^2 = k_D^2 d^2 = 4\pi\rho^*\beta^*$ and k_D is the Debye wavenumber defined by (10.2.15). The excess internal energy has a very simple form:

$$\frac{U^{ex}}{N} = -\frac{e^2}{\varepsilon d}B \tag{10.3.6}$$

and is a function of the single coupling constant ξ and not separately of ρ^* and β^*. In the high-temperature or low-density (or concentration) limit, i.e. for $\xi \ll 1$, the MSA internal energy reduces to the Debye–Hückel result:

$$\frac{U_{DH}^{ex}}{N} = -\frac{e^2}{2\varepsilon d}\xi = -\frac{k_B T}{8\pi\rho}k_D^3 \tag{10.3.7}$$

The limiting law (10.3.7) is valid when ion-size effects are negligible; it corresponds to the case when the direct correlation functions $c_{\nu\mu}(r)$ are replaced by their asymptotic forms (10.3.2) for all r. The virial pressure in the MSA is the sum of a hard-sphere contact term and the contribution of the Coulomb forces, i.e.

$$\frac{\beta P^v}{\rho} = 1 + \frac{2\pi\rho^*}{3}g_S(d) + \frac{\beta U^{ex}}{3N} \tag{10.3.8}$$

Alternatively, the pressure can be calculated by first integrating (10.3.6) to give the free energy and then differentiating with respect to density. The comparison made in Figure 10.2 for the case of a 1 : 1 electrolyte shows that the results for the excess internal energy are in good agreement with those of Monte Carlo calculations, but there is a serious inconsistency between the pressures calculated by the two different routes. In the molten-salt regime the results, not surprisingly, are much less satisfactory.[13]

Although the MSA is a good starting point for the calculation of thermodynamic properties of the restricted primitive model, it is less reliable in predicting the correlation functions. If the density and temperature are such that $\xi \gg 1$, use of the MSA leads to distribution functions $g_{11}(r)$ (or $g_{22}(r)$) that become negative at separations close to contact. The situation is improved if, at small r, the direct correlation functions $c_S(r)$ and $c_D(r)$ are allowed to deviate from their asymptotic forms.[14] In the "generalised" MSA or GMSA the deviations are expressed in terms of Yukawa functions and the closure relations for $c_S(r)$ and $c_D(r)$ in (10.3.4) are replaced by

$$c_S(r) = \frac{A_1}{r}\exp\big[-t_1(r - d)\big], \quad r > d$$

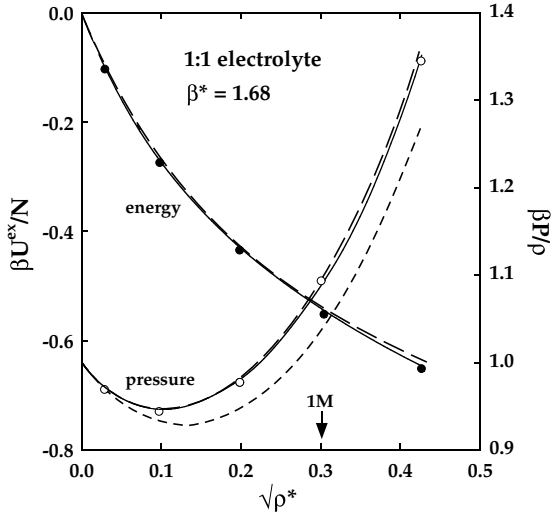

FIG. 10.2. Thermodynamic properties of the restricted primitive model of a 1 : 1 electrolyte. The points show the results of Monte Carlo simulations and the curves are calculated from the MSA and the HNC approximation. Energy: dashes, MSA; full curve, HNC. Pressure: long and short dashes, MSA via the energy and virial equations, respectively; full curve, HNC via the virial (or energy) equation. The value of β^* corresponds to an aqueous solution of ions of diameter 4.25 Å at $T = 298$ K; the arrow marks the value of $\sqrt{\rho^*}$ corresponding to a 1 M solution. After Rasaiah *et al.*[12]

$$c_{\mathrm{D}}(r) = -\frac{2\beta e^2}{\varepsilon r} - \frac{A_2}{r}\exp\bigl[-t_2(r-d)\bigr], \quad r > d \tag{10.3.9}$$

The parameters A_1, t_1, A_2 and t_2 are related through a set of algebraic equations to the internal energy, compressibility, virial pressure and contact value of $g_{\mathrm{D}}(r)$, and can be fitted to those quantities if the necessary data are available from an independent source. Where that is possible, the resulting pair distribution functions represent a significant improvement over the MSA, but in this form the theory is not self-contained.

The main appeal of theories such as the MSA or GMSA in the calculation of the pair distribution functions is the fact that they can be solved analytically in closed or nearly closed form, but their applicability is limited, at least in their conventional forms, to systems of charged hard spheres. These "primitive" models display certain structural features that are artefacts of the hard-sphere interaction. In particular, for values of ρ^* and β^* appropriate to molten salts, the main peak in the distribution functions for ions of like charge, i.e. $g_{++}(r)$ or $g_{--}(r)$, shows a marked splitting not seen experimentally. The splitting disappears when the short-range repulsion is softened, but different theoretical methods are then required. Of the integral-equation theories described in Chapter 4 the HNC approximation is far better suited to ionic systems than its PY counterpart. Equation (4.4.3) shows that the PY approximation cannot account for the exponential screening of the pair correlations at large separations, since within that approximation the pair distribution function decays as the pair potential. The HNC equation does describe the long-range correlations correctly

and there is also a close connection between HNC theory and the traditional form of the Debye–Hückel approach. When generalised to a system of more than one component, the exact relation (4.6.13) becomes

$$\ln\left[h_{\nu\mu}(r)+1\right] = -\beta v_{\nu\mu}(r) + d_{\nu\mu}(r) + h_{\nu\mu}(r) - c_{\nu\mu}(r) \tag{10.3.10}$$

and the HNC approximation corresponds to setting $d_{\nu\mu}(r) = 0$ for all pairs ν, μ. As Figure 10.2 illustrates, the thermodynamic results obtained in this way for a 1 : 1 electrolyte agree very well with those calculated by the Monte Carlo method. The degree of thermodynamic consistency in the theory is high; even at the highest concentration studied, pressures calculated via the compressibility and virial (or energy) routes differ by less than 1%. Good results are also obtained for the thermodynamic properties of the restricted primitive model of a 2 : 2 electrolyte, where the superiority of the HNC approximation over the MSA becomes more evident.[15] On the other hand, over a range of low to moderate concentrations the calculated like-ion distribution function of the 2 : 2 system has a pronounced peak at $r \approx 2d$, a feature that persists even when the hard-sphere term in the pair potential is replaced by an inverse-power repulsion.[16] No similar peak is seen in simulations of the same potential models, as the examples shown in Figure 10.3 illustrate; instead, the distribution function increases monotonically towards its limiting value at large r. Conversely, the HNC calculations significantly underestimate the height (of order 100) of the peak in the unlike-ion distribution function, the strength of which provides a measure of the degree of ion pairing in the system. These defects in the theory are linked to the difference in form of the bridge functions for like and unlike pairs. The results of simulations[16,17] show that the function $d_{++}(r)$ (or $d_{--}(r)$) is negative at all separations, and therefore resembles the bridge function of the Lennard-Jones fluid (see Figure 4.6), but $d_{+-}(r)$ is everywhere positive. Thus the HNC approximation acts in such a way as to weaken both the effective repulsion between ions of like charge and the effective attraction between those of unlike charge, with differing consequences for the calculated distribution functions.[18] At high concentrations the bridge functions maintain their difference in sign but their magnitude is greatly reduced. The error involved in neglecting them is therefore small and the spurious peak in the like-ion distribution function becomes progressively less pronounced.

The HNC approximation is also successful in reproducing the pair structure under state conditions typical of molten salts, as shown by the results for the simple molten salt plotted in Figure 10.1. The deficiencies in the approximation are evident only in the small-k region of $S_{NN}(k)$; the error there means that the calculated compressibility is about twice as large as that obtained by simulation. A systematic study of the alkali halides has confirmed that HNC theory is able to reproduce quantitatively all the main features of the pair distribution functions of more realistic potential models; still better results are obtained by including the contributions from the bridge diagrams in a semiempirical way[19] or by enforcing thermodynamic self-consistency through the hybrid, HMSA scheme[20] mentioned in Section 4.7.

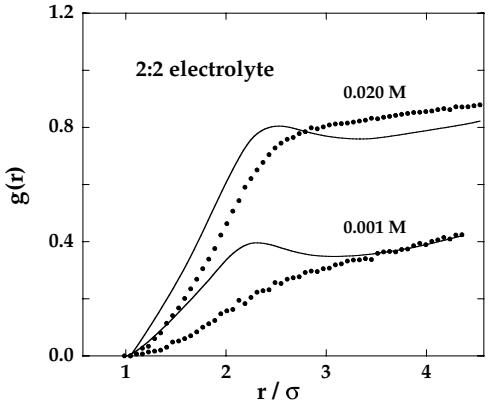

FIG. 10.3. Pair distribution function for like-charged ions in a 2:2 electrolyte solution under state conditions corresponding to an aqueous solution at $T = 298$ K. Short-range repulsions are represented by a soft-sphere (r^{-9}) potential and σ is the separation at which the cation–anion potential is a minimum. The points show the results of molecular-dynamics simulations and the curves are calculated from the HNC approximation. The spurious peak in the HNC results is less pronounced at the higher concentration and disappears for concentrations greater than about 0.06 M. After Duh and Haymet.[16]

10.4 FREQUENCY-DEPENDENT ELECTRIC RESPONSE

We have seen in earlier sections of this chapter that the static properties of ionic liquids are strongly affected by the long-range nature of the Coulomb potential or, equivalently, the k^{-2} singularity in its Fourier transform. We now turn to the question of how the same factors influence the dynamical correlations. The discussion here is limited to two-component systems of ions *in vacuo*, the case of liquid metals being deferred until Section 10.9. The phenomena of greatest interest are those linked to charge fluctuations; these generate a local electric field that acts as a restoring force on the local charge density. At low frequencies the charge density responds in a diffusive manner, but at high frequencies there is a reactive behaviour, which gives rise to a propagating mode of the type briefly discussed in Section 10.1.

The linear combinations of microscopic partial densities that arise naturally in a discussion of the collective dynamics are the mass (M) and charge (Z) densities, defined in terms of Fourier components as

$$\rho_{\mathbf{k}}^{M}(t) = \sum_{\nu} m_\nu \rho_{\mathbf{k}}^{\nu}(t), \qquad \rho_{\mathbf{k}}^{Z}(t) = \sum_{\nu} z_\nu \rho_{\mathbf{k}}^{\nu}(t) \tag{10.4.1}$$

where m_ν is the mass of an ion of species ν. With each fluctuating density we may associate a current. Thus

$$\mathbf{j}_{\mathbf{k}}^{M}(t) = \sum_{\nu} m_\nu \mathbf{j}_{\mathbf{k}}^{\nu}(t), \qquad \mathbf{j}_{\mathbf{k}}^{Z}(t) = \sum_{\nu} z_\nu \mathbf{j}_{\mathbf{k}}^{\nu}(t) \tag{10.4.2}$$

where the partial currents $\mathbf{j}_{\mathbf{k}}^{\nu}$ are given by an expression identical to (7.4.7) except that the sum on i is restricted to ions of a given species. Each current can be divided into

longitudinal (l) and transverse (t) parts in the manner of (7.4.25); the longitudinal currents satisfy equations of continuity analogous to (7.4.4). The mass current is related to the stress tensor $\boldsymbol{\Pi}_{\mathbf{k}}$ by

$$\frac{\partial}{\partial t}\mathbf{j}_{\mathbf{k}}^{M}(t) + i\mathbf{k}\cdot\boldsymbol{\Pi}_{\mathbf{k}} = 0 \tag{10.4.3}$$

where the components of $\boldsymbol{\Pi}_{\mathbf{k}}$ are given by a two-component generalisation of (8.4.14). Equation (10.4.3) shows that the time derivative of $\mathbf{j}_{\mathbf{k}}^{M}(t)$ vanishes as $k \to 0$. The mass current is therefore a conserved variable in the sense of Section 7.1, but the charge current is not. Although the total momentum of the ions is conserved, there is a continuous exchange of momentum between the two species; this momentum exchange is the source of the electrical resistivity of the fluid.

The mass and charge densities can be used to construct three, independent, time-correlation functions $F_{AB}(k,t)$ (with $A, B = M$ or Z), the definitions of which are similar to that of the intermediate scattering function (7.4.20). The initial values of the correlation functions are equal to the static structure factors in (10.2.2), but with number N replaced by mass M, and their Fourier transforms with respect to t are the corresponding dynamic structure factors. A function of particular interest for our purposes is the charge–charge dynamic structure factor, defined as

$$S_{ZZ}(k,\omega) = \frac{1}{2\pi N}\int_{-\infty}^{\infty}\left\langle \rho_{\mathbf{k}}^{Z}(t)\rho_{-\mathbf{k}}^{Z}\right\rangle \exp(i\omega t)\,\mathrm{d}t \tag{10.4.4}$$

Finally, three longitudinal and three transverse current correlation functions can be defined through straightforward generalisations of (7.4.25):

$$C_{AB,l}(k,t) = \frac{k^2}{N}\left\langle j_{\mathbf{k}}^{Az}(t)\, j_{-\mathbf{k}}^{Bz}\right\rangle \tag{10.4.5a}$$

$$C_{AB,t}(k,t) = \frac{k^2}{N}\left\langle j_{\mathbf{k}}^{Ax}(t)\, j_{-\mathbf{k}}^{Bx}\right\rangle \tag{10.4.5b}$$

where, as usual, the z-axis is chosen parallel to $\mathbf{k}$. Each $C_{AB,l}(k,t)$ is related to the corresponding $F_{AB}(k,t)$ by an analogue of (7.4.26).

We next consider how the response of the system to an external electric field can be described in terms of the correlation functions introduced above. This requires a generalisation to frequency-dependent perturbations of the result in (10.2.6). As an extension of the linear-response relation (7.6.26), we find that the mean induced charge density is

$$\delta\hat{\rho}_Z(\mathbf{k},t) = \left\langle \rho_{\mathbf{k}}^{Z}(t)\right\rangle = \chi_{ZZ}(k,\omega)e\phi_{\mathbf{k}}^{\mathrm{ext}}\exp(-i\omega t) \tag{10.4.6}$$

The imaginary part of the complex dynamic susceptibility $\chi_{ZZ}(k,\omega)$ is related to the dynamic structure factor $S_{ZZ}(k,\omega)$ through a trivial modification of the fluctuation–dissipation theorem (7.6.28), i.e.

$$S_{ZZ}(k,\omega) = -\frac{k_{\mathrm{B}}T}{\pi\rho\omega}\chi_{ZZ}''(k,\omega) \tag{10.4.7}$$

and the susceptibility can also be expressed in terms of the complex dielectric function $\varepsilon(k,\omega)$ by a frequency-dependent generalisation of (10.2.11):

$$\frac{1}{\varepsilon(k,\omega)} = 1 + \frac{4\pi e^2}{k^2}\chi_{ZZ}(k,\omega) \tag{10.4.8}$$

The functions $\chi_{ZZ}(k,\omega)$ and $1/\varepsilon(k,\omega)$ measure the linear response of a fluid of charged particles to an external electric field. The external field polarises the fluid and the local, internal field (the Maxwell field) is the sum of the field due to the external charge distribution and that due to the induced charge density. The local field is, of course, the field experienced by the ions. The response of the system to the local electric potential is described by a screened response function $\chi^{\rm sc}_{ZZ}(k,\omega)$, defined through the expression

$$\delta\hat{\rho}_Z(\mathbf{k},t) = \chi^{\rm sc}_{ZZ}(k,\omega)e\left[\phi^{\rm ext}_{\mathbf{k}}\exp(-i\omega t) + \delta\hat{\phi}^{\rm ind}(\mathbf{k},\omega)\right] \tag{10.4.9}$$

where the induced electric potential $\delta\hat{\phi}^{\rm ind}(\mathbf{k},\omega)$ is related to the induced charge density by Poisson's equation (cf. (10.2.5)):

$$\delta\hat{\phi}^{\rm ind}(\mathbf{k},\omega) = \frac{4\pi e}{k^2}\delta\hat{\rho}_Z(\mathbf{k},\omega) \tag{10.4.10}$$

Comparison of (10.4.9) with (10.4.6) shows that the relation between the external and screened susceptibilities is

$$\chi_{ZZ}(k,\omega) = \frac{\chi^{\rm sc}_{ZZ}(k,\omega)}{1 - \dfrac{4\pi e^2}{k^2}\chi^{\rm sc}_{ZZ}(k,\omega)} \tag{10.4.11}$$

and hence, from (10.4.8), that

$$\varepsilon(k,\omega) = 1 - \frac{4\pi e^2}{k^2}\chi^{\rm sc}_{ZZ}(k,\omega) \tag{10.4.12}$$

The response function $\chi_{ZZ}(k,\omega)$ satisfies the Kramers–Kronig relations (7.6.37) and (7.6.38), which are merely consequences of causality. The same is not necessarily true of the screened function $\chi^{\rm sc}_{ZZ}(k,\omega)$, which determines the response of the system to the local field. Since the local field depends on the material properties of the system, it cannot be controlled at will in an experiment.

The electric response of an ionic fluid can also be discussed in terms of the induced electric current. Let $\mathbf{E}(\mathbf{k},\omega)$ be a Fourier component of the local electric field. Ohm's Law in its most general form states that the induced electric current $\mathbf{J}^Z$ is linearly related to the field, i.e.

$$\mathbf{J}^Z(\mathbf{k},\omega) = \boldsymbol{\sigma}(\mathbf{k},\omega)\cdot\mathbf{E}(\mathbf{k},\omega) \tag{10.4.13}$$

The quantity $\boldsymbol{\sigma}$ is the conductivity tensor, which can be divided into longitudinal and transverse parts in the form

$$\boldsymbol{\sigma}(\mathbf{k},\omega) = \frac{\mathbf{kk}}{k^2}\sigma_l(\mathbf{k},\omega) + \left(\boldsymbol{I} - \frac{\mathbf{kk}}{k^2}\right)\sigma_t(\mathbf{k},\omega) \tag{10.4.14}$$

where σ_l and σ_t are scalars. The longitudinal and transverse projections of the induced current are related, respectively, to the longitudinal (or irrotational) and transverse (or divergence-free) components of the local electric field. Thus

$$\mathbf{J}_l^Z(\mathbf{k},\omega) = \sigma_l(\mathbf{k},\omega)\mathbf{E}_l(\mathbf{k},\omega), \qquad \mathbf{J}_t^Z(\mathbf{k},\omega) = \sigma_t(\mathbf{k},\omega)\mathbf{E}_t(\mathbf{k},\omega) \tag{10.4.15}$$

Since $\mathbf{E} = -\nabla\delta\phi$, it follows that the component $\mathbf{E}_l(\mathbf{k},\omega)$ of the local field is related to the total electric potential by the expression

$$\mathbf{E}_l(\mathbf{k},\omega) = -i\mathbf{k}\delta\hat{\phi}(\mathbf{k},\omega) = -i\mathbf{k}\left[\phi_{\mathbf{k}}^{\text{ext}}\exp(-i\omega t) + \delta\hat{\phi}^{\text{ind}}(\mathbf{k},\omega)\right] \tag{10.4.16}$$

Equations (7.4.4), (10.4.9), (10.4.12), (10.4.15) and (10.4.16) can now be combined to yield the fundamental relation between the dielectric function and the conductivity tensor:

$$\varepsilon(k,\omega) = 1 + \frac{4\pi i}{\omega}\sigma_l(k,\omega) \tag{10.4.17}$$

Note that $\sigma_l(k,\omega)$ is a screened response function in the same sense as $\chi_{ZZ}^{\text{sc}}(k,\omega)$, since it measures a response to the internal field.

Linear-response theory was used in Section 7.7 to derive a microscopic expression for the frequency-dependent electrical conductivity; this "external" conductivity measures the response of a fluid to a uniform ($\mathbf{k} = 0$) applied electric field. A uniform field corresponds to a situation in which the boundaries of the system are removed to infinity, thereby avoiding the appearance of a surface polarisation. The electric response to an inhomogeneous ($\mathbf{k}$-dependent) applied field is measured by a wavenumber-dependent external conductivity that can be related to the time-autocorrelation function of the fluctuating charge current $\mathbf{j}_{\mathbf{k}}^Z(t)$. In the case of the longitudinal component the required generalisation of (7.7.10) is simply

$$\sigma_l^{\text{ext}}(k,\omega) = \frac{\beta e^2}{V}\int_0^\infty \left\langle j_{\mathbf{k}}^{Zz}(t)\, j_{-\mathbf{k}}^{Zz}\right\rangle \exp(i\omega t)\,\mathrm{d}t \tag{10.4.18}$$

However, the macroscopic electrical conductivity σ given by the low-frequency limit of (7.7.10) is not the same as the $k,\ \omega \to 0$ limit of $\sigma_l^{\text{ext}}(k,\omega)$. Indeed, it follows from the continuity equation (see (7.4.4)) that the integral in (10.4.18) can be re-expressed as

$$\begin{aligned}\int_0^\infty \left\langle j_{\mathbf{k}}^{Zz}(t)\, j_{-\mathbf{k}}^{Zz}\right\rangle \exp(i\omega t)\,\mathrm{d}t &= \frac{1}{k^2}\int_0^\infty \left\langle \dot{\rho}_{\mathbf{k}}^{Z}(t)\,\dot{\rho}_{-\mathbf{k}}^{Z}\right\rangle \exp(i\omega t)\,\mathrm{d}t \\ &= \frac{-i\omega N S_{ZZ}(k) + \omega^2 N\widetilde{F}_{ZZ}(k,\omega)}{k^2}\end{aligned} \tag{10.4.19}$$

Written in this form it is easy to see that the integral vanishes as $k,\ \omega \to 0$, since $S_{ZZ}(k) \sim k^2$ for small k. (Note that $\widetilde{F}_{ZZ}(k,\omega)$ is the Laplace transform of $F_{ZZ}(k,t)$, which is bounded above by $S_{ZZ}(k)$: see (7.1.14).) On the other hand, the rotational invariance of an isotropic fluid implies that the macroscopic longitudinal and transverse conductivities must be the same, i.e. $\sigma_l^{\text{ext}}(0,\omega) = \sigma_t^{\text{ext}}(0,\omega) = \sigma(\omega)$. Hence σ may be defined in terms of the transverse charge–current autocorrelation function; the transverse current is not related to the charge density by a continuity equation and is therefore unaffected by the small-k divergence of the longitudinal electric field. Thus

$$\begin{aligned}\sigma &= \lim_{\omega\to 0}\lim_{k\to 0}\frac{\beta e^2}{V}\int_0^\infty \left\langle j_{\mathbf{k}}^{Zx}(t)\, j_{-\mathbf{k}}^{Zx}\right\rangle \exp(i\omega t)\,\mathrm{d}t \\ &= \lim_{\omega\to 0}\lim_{k\to 0}\frac{\beta\rho e^2}{k^2}\widetilde{C}_{ZZ,t}(k,\omega) \end{aligned} \tag{10.4.20}$$

The differing behaviour of the longitudinal and transverse charge–current autocorrelation functions is also evident from the sum rules for the corresponding spectra. The short-time expansions of $C_{ZZ,l}(k,t)$ and $C_{ZZ,t}(k,t)$ can be written in a form similar to (7.4.31) and (7.4.36), namely

$$C_{ZZ,l}(k,t) = \omega_0^2\left(1 - \omega_{1l}^2\frac{t^2}{2!} + \cdots\right) \tag{10.4.21a}$$

$$C_{ZZ,t}(k,t) = \omega_0^2\left(1 - \omega_{1t}^2\frac{t^2}{2!} + \cdots\right) \tag{10.4.21b}$$

where, in the case when $z_1 = -z_2 = z$:

$$\omega_0^2 = z^2k^2\left(\frac{k_{\mathrm{B}}T}{2M}\right) \tag{10.4.22}$$

with $M = m_1m_2/(m_1+m_2)$. The frequency moments ω_{1l}^2 and ω_{1t}^2 are the charge–current analogues of the quantities defined in Section 7.4. If the interionic potentials are separated into their coulombic and short-range parts, the derivation of (7.4.35) and (7.4.38) can be suitably generalised.[21] The resulting expressions are lengthy, but reduce in the limit $k \to 0$ to the simpler forms given by

$$\lim_{k\to 0}\omega_{1l}^2(k) = \tfrac{2}{3}\omega_{\mathrm{p}}^2 + \frac{\rho}{6M}\int \nabla^2 v_{12}^{\mathrm{S}}(r)\, g_{12}(r)\,\mathrm{d}\mathbf{r} \tag{10.4.23a}$$

$$\lim_{k\to 0}\omega_{1t}^2(k) = -\tfrac{1}{3}\omega_{\mathrm{p}}^2 + \frac{\rho}{6M}\int \nabla^2 v_{12}^{\mathrm{S}}(r)\, g_{12}(r)\,\mathrm{d}\mathbf{r} \tag{10.4.23b}$$

where $v_{12}^{\mathrm{S}}(r)$ is the short-range part of the cation–anion potential and ω_{p} is the plasma frequency (10.1.8), generalised to the two-component case:

$$\omega_{\mathrm{p}}^2 = \sum_{\nu} \frac{4\pi\rho_\nu z_\nu^2 e^2}{m_\nu} \tag{10.4.24}$$

Thus, in contrast to the results obtained in Section 7.4, the characteristic frequencies of the charge–current fluctuations remain non-zero as $k \to 0$. In addition, the longitudinal and transverse frequencies at $\mathbf{k} = 0$ are split according to the rule

$$\omega_{1l}^2(0) - \omega_{1t}^2(0) = \omega_{\mathrm{p}}^2 \tag{10.4.25}$$

This result is of the same form as the well-known relation between the longitudinal and transverse optic frequencies of ionic crystals. The behaviour of $\omega_{1l}(k)$ and $\omega_{1t}(k)$ at finite wavelengths is also similar to that of the corresponding phonon dispersion curves for the crystal: initially, $\omega_{1l}(k)$ falls rapidly with increasing k, but the curve of $\omega_{1t}(k)$ is almost flat. In the case of the alkali halides, $\omega_{1l}(0)$ is typically 20–30% larger than ω_{p}.

The nature of the collective modes associated with fluctuations in mass, charge and temperature in a molten salt can be analysed by methods described in Chapters 8 and 9. By analogy with the phonon spectra of ionic crystals, the collective modes are expected to be of acoustic and optic character, corresponding to low-frequency sound waves and high-frequency "plasma" oscillations. The different fluctuations are, in general, strongly coupled, and the associated memory functions have a complicated structure. A considerable simplification occurs when the anions and cations differ only in the sign of their electrical charge. Under such conditions, charge fluctuations are completely decoupled from fluctuations in mass and temperature at all frequencies and all wavenumbers. The same is true for any molten salt in the long-wavelength limit, thereby making it possible to calculate the spectrum of charge fluctuations at long wavelengths by the following, simple, macroscopic argument.[9] The Laplace transform of the continuity equation for the induced charge density is

$$-i\omega\delta\tilde{\rho}_Z(\mathbf{k},\omega) = \delta\hat{\rho}_Z(\mathbf{k},t=0) + i\mathbf{k}\cdot\mathbf{J}^Z(\mathbf{k},\omega) \tag{10.4.26}$$

while Poisson's equation may be written as

$$-i\mathbf{k}\cdot\mathbf{E}(\mathbf{k},\omega) = 4\pi\delta\tilde{\rho}_Z(\mathbf{k},\omega) \tag{10.4.27}$$

These two expressions can be combined with the longitudinal projection of Ohm's Law to give

$$\delta\tilde{\rho}_Z(\mathbf{k},\omega) = \frac{\delta\hat{\rho}_Z(\mathbf{k},t=0)}{-i\omega + 4\pi\sigma_l(k,\omega)} \tag{10.4.28}$$

If we multiply (10.4.28) through by $\delta\hat{\rho}_Z(-\mathbf{k},t=0)$ and take the thermal average, we find that

$$\widetilde{F}_{ZZ}(k,\omega) = \frac{S_{ZZ}(k)}{-i\omega + 4\pi\sigma_l(k,\omega)} \tag{10.4.29}$$

In the limit $k \to 0$, $\sigma_l(k, \omega)$ can be replaced by $\sigma(\omega)$. This gives an important result:

$$\lim_{k\to 0} \frac{\widetilde{F}_{ZZ}(k,\omega)}{S_{ZZ}(k)} = \frac{1}{-i\omega + 4\pi\sigma(\omega)} \tag{10.4.30}$$

Comparison with (7.3.23) shows that the frequency-dependent, complex conductivity is the memory function for the long-wavelength limit of the charge-density autocorrelation function. The spectrum of charge-density fluctuations may therefore be expressed in terms of the real (σ') and imaginary (σ'') parts of $\sigma(\omega)$ in the form

$$\lim_{k\to 0} \frac{S_{ZZ}(k,\omega)}{S_{ZZ}(k)} = \frac{1}{\pi} \frac{4\pi\sigma'(\omega)}{[\omega - 4\pi\sigma''(\omega)]^2 + [4\pi\sigma'(\omega)]^2} \tag{10.4.31}$$

In the low-frequency limit, $\sigma'(\omega) \to \sigma$, $\sigma''(\omega) \to 0$, and (10.4.31) reduces to

$$S_{ZZ}(k,\omega) \sim \frac{1}{\pi} \frac{4\pi\sigma(k/k_{\mathrm{D}})^2}{\omega^2 + (4\pi\sigma)^2}, \quad k, \omega \to 0 \tag{10.4.32}$$

Charge fluctuations in the low-frequency, long-wavelength regime are therefore of a non-propagating type. The same is true of concentration fluctuations in a mixture of uncharged particles, but the two cases differ in a significant way. If the coupling to other hydrodynamic variables is weak, a Fourier component of a fluctuation in the local concentration $c(\mathbf{r}, t)$ in a non-ionic, binary mixture decays in approximately the same way as a component of the density of tagged particles in a one-component system (see (8.2.5)), i.e.

$$c_{\mathbf{k}}(t) \approx c_{\mathbf{k}} \exp\left(-Dk^2 t\right) \tag{10.4.33}$$

where D is the interdiffusion coefficient.[22] The spectrum of concentration fluctuations therefore has approximately the same functional form as the self dynamic structure factor (8.2.9):

$$\begin{aligned} S_{cc}(k,\omega) &= \frac{1}{2\pi} \int_{-\infty}^{\infty} \left\langle c_{\mathbf{k}}(t) c_{-\mathbf{k}} \right\rangle \exp(i\omega t)\, \mathrm{d}t \\ &\approx \frac{\langle |c_{\mathbf{k}}|^2 \rangle}{\pi} \frac{Dk^2}{\omega^2 + (Dk^2)^2} \end{aligned} \tag{10.4.34}$$

Equation (10.4.34) represents a lorentzian curve centred at $\omega = 0$ and having a width that varies as k^2, whereas the width of the charge-fluctuation spectrum (10.4.32) remains non-zero even in the long-wavelength limit. The source of this difference in behaviour is the fact that in the coulombic case the "restoring force" is proportional to the charge-density fluctuation, while in the neutral system it is proportional to the laplacian of the concentration fluctuation.

Although the hydrodynamic analysis yields the correct low-frequency behaviour, the possibility that a propagating charge-density oscillation could occur at higher frequencies has to be investigated within the framework either of generalised hydrodynamics or of the

memory-function formalism. In particular, the memory-function representations developed in Sections 9.3 and 9.4 lend themselves easily to a unified treatment of transverse and longitudinal charge fluctuations. Here, however, we consider only the more interesting question of the nature of the longitudinal fluctuations. We also restrict the discussion to long wavelengths and to the case when $z_1 = -z_2 = z$, and use the fact that

$$\lim_{k\to 0} \frac{\omega_0^2}{S_{ZZ}(k)} = \omega_\mathrm{p}^2 \tag{10.4.35}$$

which follows from the long-wavelength relation (10.2.14) and the definitions (10.4.22) and (10.4.24). When adapted to the problem of the longitudinal charge current, the memory-function equation (9.4.7) becomes

$$\widetilde{C}_{ZZ,l}(k,\omega) = \frac{\omega_0^2}{-i\omega + \dfrac{\omega_\mathrm{p}^2}{-i\omega} + \widetilde{N}_l(k,\omega)} \tag{10.4.36}$$

Use of (10.4.19) shows that the corresponding expression for the charge-density autocorrelation function is given in terms of Laplace transforms by

$$\widetilde{F}_{ZZ}(k,\omega) = \frac{S_{ZZ}(k)}{-i\omega + \dfrac{\omega_\mathrm{p}^2}{-i\omega + \widetilde{N}_l(k,\omega)}} \tag{10.4.37}$$

The high-frequency behaviour can now be studied in an approximate way by assuming that the memory function $N_l(k,t)$ decays exponentially with a relaxation time equal τ_l. This is the characteristic approximation of the viscoelastic model introduced in Chapter 9, and leads, for small k, to

$$\widetilde{N}_l(k,\omega) = \frac{\omega_{1l}^2 - \omega_\mathrm{p}^2}{-i\omega + 1/\tau_l} \tag{10.4.38}$$

A simple calculation then shows that if $\omega\tau_l \gg 1$, the charge–charge dynamic structure factor (proportional to $\mathrm{Re}\,\widetilde{F}_{ZZ}(k,\omega)$) has peaks at $\omega = 0$ and $\omega = \pm\omega_{1l}$; those at $\pm\omega_{1l}$ correspond to charge fluctuations that propagate at a frequency comparable with the plasma frequency, but modified by the short-range interactions between ions. The calculation is a crude one, limited as it is to high frequencies and long wavelengths, but it provides a fair description of the dispersion of the propagating mode observed in simulations (see below in Figure 10.5).

10.5 MICROSCOPIC DYNAMICS IN MOLTEN SALTS

Much of our current understanding of the microscopic dynamics in strongly coupled ionic systems comes from molecular-dynamics simulations. In this section we give some examples, taken from studies of monovalent molten salts, that illustrate the richness of the observed single-particle and collective behaviour.

Single-particle motion is conveniently discussed in terms of the velocity autocorrelation functions $Z_\nu(t)$ and self-diffusion coefficients D_ν of the two ionic species; D_ν is related to $Z_\nu(t)$ in the manner of (7.2.7). For mixtures of neutral particles in which cross correlations of velocity of the type $\langle \mathbf{u}_i(t) \cdot \mathbf{u}_j \rangle$ $(i \neq j)$ are negligible, the two self-diffusion coefficients are related to the interdiffusion coefficient D by the expression

$$D \approx \mathcal{F} \frac{x_1 x_2}{N k_B T} (x_2 D_1 + x_1 D_2) \tag{10.5.1}$$

where $\mathcal{F} = (\partial^2 G / \partial x_1^2)_{P,T}$ is a purely thermodynamic quantity.[22] If, in addition, the mixture is nearly ideal, which is a good approximation for mixtures of simple liquids, $\mathcal{F} \approx N k_B T / x_1 x_2$, and (10.5.1) becomes

$$D \approx x_2 D_1 + x_1 D_2 \tag{10.5.2}$$

In an ionic liquid interdiffusion is equivalent to electrical conduction. We have shown in Section 7.7 that the static electrical conductivity σ is proportional to the time integral of the electric-current autocorrelation function $J(t)$, defined as

$$J(t) = \langle \mathbf{j}^Z(t) \cdot \mathbf{j}^Z \rangle = \sum_{i=1}^{N} \sum_{j=1}^{N} \langle z_i \mathbf{u}_i(t) \cdot z_j \mathbf{u}_j \rangle \tag{10.5.3}$$

If the self-correlation terms $(i = j)$ in (10.5.3) are separated from the cross terms $(i \neq j)$, integration over time and use of (7.7.10) shows that

$$\sigma = \beta e^2 \rho \left(x_1 z_1^2 D_1 + x_2 z_2^2 D_2 \right) (1 - \Delta) \tag{10.5.4}$$

Equation (10.5.4), with $\Delta = 0$, is called the Nernst–Einstein relation; the value of the deviation factor Δ is a measure of the importance of cross-correlations. If $\Delta = 0$, (10.5.4) becomes the ionic equivalent of the approximate relation (10.5.2). In practice, at least for the alkali halides, Δ is significantly different from zero and always positive. The importance of cross correlations in monovalent salts is illustrated in Figure 10.4, where molecular-dynamics results for the velocity and electric-current autocorrelation functions of the simple molten salt are plotted. The symmetry of the model means that the velocity autocorrelation functions of cations and anions are identical; if cross-correlations of velocities were negligible, the normalised curves of $Z(t)$ and $J(t)$ would also be the same. At short times, however, there are substantial differences between the two functions, and the calculated Nernst–Einstein deviation factor for the case shown is $\Delta = 0.19$. The positive value of Δ corresponds physically to the fact that motion in the same direction by a pair of oppositely charged ions contributes to self-diffusion but not to electrical conduction. The numerical result agrees well with experimental data: the mean value of Δ for eight alkali-halide salts is 0.26. The observed deviations from the Nernst–Einstein relation therefore have a natural explanation in terms of positive correlations between the velocities of nearest-neighbour ions that persist for times which, for a real molten salt, would be of order 10^{-12} s. Such

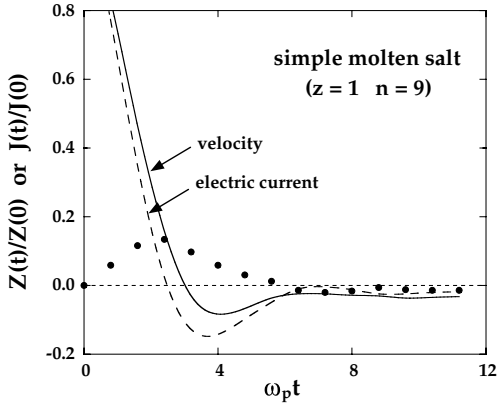

FIG. 10.4. Normalised velocity and electric-current autocorrelation functions of the simple molten salt[10] under the state conditions described in the caption to Figure 10.1. Full curve: $Z(t)/Z(0)$; dashes: $J(t)/J(0)$. The points show the difference between the two functions.

correlations are of a nature that physical intuition would lead one to expect, but it is not necessary to assume the existence of well-defined ion pairs.

The velocity autocorrelation function shown in Figure 10.4 has a negative plateau similar to that seen in argon-like liquids. Both the shape of $Z(t)$ and the value of the diffusion coefficient are reasonably well reproduced by a mode-coupling calculation[23] of the type discussed in Section 9.5. The mode-coupling results for the electric-current autocorrelation function are much less satisfactory and the theoretical value for the case illustrated in the figure is about 30% too small. These discrepancies have been attributed to the neglect of temperature fluctuations in the mode-coupling calculations.

Molecular-dynamics results on self diffusion are also available for rigid-ion models of the alkali halides in which allowance is made for the differences in mass and size of the two ions. Where the mass difference is large, the velocity autocorrelation function of the lighter ion is strongly oscillatory. This effect is the result of a "rattling" motion of the ion in the relatively long-lived cage formed by its heavier neighbours and is particularly marked in the case of the very light Li^+ ion. The calculated diffusion coefficients are in general smaller than the experimental values, sometimes significantly so, but the agreement with experiment is substantially improved when allowance is made for polarisation of the ions.[24] In a rigid-ion model, local charge neutrality around a diffusing ion can be maintained only by bodily displacement of its neighbours; when the ions are polarisable, an additional screening mechanism is present that does not entail movement of the ion cores. The net result is that the cage effect is smaller for polarisable ions; this leads to an increased damping of oscillations in the velocity-autocorrelation function and a consequent increase in the diffusion coefficient.

The wavenumber-dependent collective motions in molten salts have also been studied by molecular dynamics. The simple molten salt is particularly well-suited to theoretical investigation of the collective modes,[10] because the fluctuations in mass and charge densities are strictly independent at all wavelengths (see Section 10.4). The main objects of interest are the optic-type modes associated with charge fluctuations, since these are specific to ionic

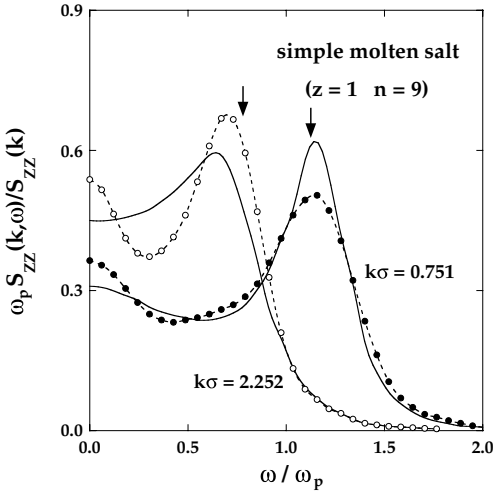

FIG. 10.5. Charge–charge dynamic structure factor of the simple molten salt[10] at two values of k under the state conditions described in the caption to Figure 10.1. The points show the results of molecular-dynamics calculations, the dashes are guides to the eye and the curves are calculated from a single-relaxation time approximation for the memory function $N_l(k,t)$, with the relaxation time determined by a least-squares fit to the simulated spectra. The arrows mark the value of $\omega_{1l}(k)$.

fluids. The results of the simulations show that the charge-density autocorrelation function $F_{ZZ}(k,t)$ is strongly oscillatory at wavelengths up to about twice the mean interionic spacing. These oscillations give rise to a "plasmon" peak in the dynamic structure factor $S_{ZZ}(k,\omega)$, as shown in Figure 10.5. The frequency ω_k at which the optic peak is seen is in the region of the plasma frequency ω_p, but its dispersion is strongly negative and described reasonably well by the relation $\omega_k \approx \omega_{1l}(k)$, as suggested by the rough calculation made in the previous section. The peak eventually disappears at a value of k close to the position of the main peak in the charge–charge structure factor $S_{ZZ}(k)$. More surprising is the fact that at small wavenumbers the optic peak initially sharpens as k increases, i.e. the damping of the plasmon mode becomes weaker. This behaviour is in striking contrast to that of the sound-wave mode; in molten salts, as in systems of neutral particles, the sound-wave damping increases rapidly with k.

The main features of the charge-fluctuation spectrum of the simple molten salt are also seen in simulations of more realistic rigid-ion models; the effect of including polarisation is to broaden the optic peak and shift it to lower frequencies.[25] It can be seen from Figure 10.5 that in the case of the simple molten salt the single-relaxation time, viscoelastic approximation cannot account for the detailed shape of the spectrum. At least two relaxation times are required, and other calculations have confirmed that the memory function for the longitudinal charge–current correlation function consists of a rapidly decaying term and a long-time, quasi-exponential tail; it therefore has a structure similar to that required to describe the density fluctuations in argon-like liquids (see Section 9.4). A fair description of the spectra of mass and charge fluctuations in the simple molten salt has been obtained by mode-coupling methods along the general lines of Section 9.5. In particular, a mode-

coupling calculation[26] has shown that the width of the plasmon peak should decrease with increasing k in a certain wavenumber range, in qualitative agreement with the unexpected behaviour observed in the simulations.

Several attempts have been made to detect a collective, plasmon-like excitation in molten salts by inelastic neutron scattering. If b_1 and b_2 are the coherent neutron scattering lengths of the two ionic species, and if $z_1 = -z_2$, a straightforward extension of the derivation given for a one-component fluid in Section 7.5 shows that the coherent, inelastic cross-section for a monovalent salt can be written in the form

$$\frac{\mathrm{d}^2\sigma}{\mathrm{d}\Omega\,\mathrm{d}\omega} \propto (b_1+b_2)^2 S_{NN}(k,\omega) + 2\left(b_1^2 - b_2^2\right) S_{NZ}(k,\omega) + (b_1-b_2)^2 S_{ZZ}(k,\omega) \tag{10.5.5}$$

Thus a single experiment yields only a linear combination of the three dynamic structure factors (number–number, number–charge and charge–charge). Moreover, the contribution made by the charge-fluctuation component is very low at small wavenumbers, since $S_{ZZ}(k)$ (the integral of $S_{ZZ}(k,\omega)$) is proportional to k^2 in the limit $k \to 0$. Only when the scattering lengths are such that $b_1 \approx -b_2$ does the component $S_{ZZ}(k,\omega)$ dominate, and this situation is not easily achievable with readily available isotopes. The most convincing experimental evidence obtained so far for the existence of a plasmon mode in ionic liquids comes from the analysis of infrared reflectivity data for molten lithium fluoride.[27] The resulting spectrum, which corresponds effectively to $S_{ZZ}(k,\omega)$ at zero wavenumber, displays a well-defined plasmon-like response, at a frequency somewhat above ω_p, which is well separated from a central, diffusive peak.

The autocorrelation functions of the transverse components of the mass and charge currents have been calculated in molecular-dynamics simulations of a number of model systems. The frequency of the transverse optic mode lies roughly an amount ω_p below that of its longitudinal counterpart, as suggested by the sum rule (10.4.25), and is relatively insensitive to wavenumber. As in the case of the longitudinal modes, an accurate memory-function fit of the transverse-current spectra requires the introduction of two relaxation times that are very different in value.[25]

10.6 THE ELECTRIC DOUBLE LAYER

So far in this chapter the emphasis has been placed on the bulk properties of ionic liquids. In this section and the one that follows we discuss some of the new phenomena that arise in the vicinity of a charged surface, and show how the resulting inhomogeneities can be described within the framework of the density-functional theory developed in Chapters 3 and 6.

When colloidal particles or macromolecules are dissolved in a highly polar solvent such as water, they will normally release counterions into the solvent, leaving behind a "polyion" carrying a surface charge of opposite sign. The solvent will in general be an electrolyte solution, and itself is therefore a source of both counterions and coions, coions being those of like charge to that of the polyion. Counterions are attracted by the surface charge, but

the effect is counterbalanced by the tendency for ions to spread into the bulk solution in order to maximise the entropy. These competing effects lead to the formation of an electric double layer at the charged surface, to which both coions and counterions contribute. In the discussion that follows we restrict ourselves to the situation in which only two ionic species are present, with charges $z_\nu e$, $\nu = +$ or $-$. The inhomogeneous solution in the vicinity of the charged surface is assumed to be in chemical equilibrium with a bulk solution (or reservoir) of the same ions at chemical potentials, μ_ν. The surface charge is the source of an external field acting on the ions and the solution of the electrostatic problem involves boundary conditions on the local electrostatic field.

Within a confined dielectric medium of permittivity ε, the electrostatic potential at $\mathbf{r}'$ due to a unit point charge at $\mathbf{r}$ is given by the Green's function $\mathcal{G}(\mathbf{r}, \mathbf{r}')$ that satisfies Poisson's equation:

$$\nabla^2 \mathcal{G}(\mathbf{r}, \mathbf{r}') = -\frac{4\pi}{\varepsilon}\delta(\mathbf{r}' - \mathbf{r}) \tag{10.6.1}$$

for given boundary conditions at any interfaces.[28] If there are no boundaries, the Green's function is the usual Coulomb potential, $\mathcal{G}(\mathbf{r}, \mathbf{r}') = \mathcal{G}(\mathbf{r}' - \mathbf{r}) = 1/\varepsilon|\mathbf{r}' - \mathbf{r}|$; when boundaries are present, the solution can be obtained by the method of images, at least for sufficiently simple geometries.[29] Let $\rho_Z(\mathbf{r})$ be the local charge density of the fluid, defined as[30]

$$\rho_Z(\mathbf{r}) = \sum_\nu z_\nu \rho_\nu^{(1)}(\mathbf{r}) \tag{10.6.2}$$

where $\rho_\nu^{(1)}(\mathbf{r})$ is the single-particle density of species ν. The local electrostatic potential $\Phi^{\mathrm{C}}(\mathbf{r})$ that satisfies Poisson's equation:

$$\nabla^2 \Phi^{\mathrm{C}}(\mathbf{r}) = -\frac{4\pi e}{\varepsilon}\rho_Z(\mathbf{r}) \tag{10.6.3}$$

subject to any boundary conditions, is

$$\Phi^{\mathrm{C}}(\mathbf{r}) = \int \mathcal{G}(\mathbf{r}, \mathbf{r}') e \rho_Z(\mathbf{r}')\, \mathrm{d}\mathbf{r}' \tag{10.6.4}$$

The electrostatic energy of the system is then given by

$$U^{\mathrm{C}} = \tfrac{1}{2} e \int \Phi^{\mathrm{C}}(\mathbf{r}) \rho_Z(\mathbf{r})\, \mathrm{d}\mathbf{r} = \tfrac{1}{2} e^2 \iint \rho_Z(\mathbf{r}) \mathcal{G}(\mathbf{r}, \mathbf{r}') \rho_Z(\mathbf{r}')\, \mathrm{d}\mathbf{r}\, \mathrm{d}\mathbf{r}' \tag{10.6.5}$$

where the integral extends over the region occupied by the fluid. From now on, however, we shall restrict ourselves to the situation in which there are no dielectric discontinuities and the permittivity is the same throughout space. Lifting this restriction introduces only technical complications.

The grand, potential functional of the fluid is

$$\Omega\big[\rho_+^{(1)}, \rho_-^{(1)}\big] = \mathcal{F}\big[\rho_+^{(1)}, \rho_-^{(1)}\big] - \sum_\nu \int \big[\mu_\nu - \phi_\nu(\mathbf{r})\big] \rho_\nu^{(1)}(\mathbf{r})\, \mathrm{d}\mathbf{r} \tag{10.6.6}$$

where $\phi_\nu(\mathbf{r})$ is the total external potential acting on ions of species ν, which may have both coulombic and non-coulombic components. The intrinsic free-energy functional $\mathcal{F}$ can be split, as usual, into ideal and excess parts:

$$\mathcal{F}\big[\rho_+^{(1)}, \rho_-^{(1)}\big] = \sum_\nu \mathcal{F}_\nu^{\mathrm{id}}\big[\rho_\nu^{(1)}\big] + \mathcal{F}^{\mathrm{ex}}\big[\rho_+^{(1)}, \rho_-^{(1)}\big] \tag{10.6.7}$$

where the ideal contributions are defined as in (3.1.22) and the excess contribution is given by a two-component generalisation of (3.5.23). If the reference state, corresponding to $\lambda = 0$ in (3.5.23), is taken as one in which the chemical potentials are the same as those of the bulk solution, then

$$\begin{aligned}\mathcal{F}^{\mathrm{ex}}&\big[\rho_+^{(1)}, \rho_-^{(1)}\big] \\ &= F^{\mathrm{ex}}(n_+, n_-) + \sum_\nu \mu_\nu^{\mathrm{ex}} \int \Delta\rho_\nu^{(1)}(\mathbf{r})\,\mathrm{d}\mathbf{r} \\ &\quad - k_{\mathrm{B}}T \sum_\nu \sum_\mu \int_0^1 \mathrm{d}\lambda\,(1-\lambda) \iint \Delta\rho_\nu^{(1)}(\mathbf{r}) c_{\nu\mu}(\mathbf{r}, \mathbf{r}'; \lambda) \Delta\rho_\mu^{(1)}(\mathbf{r}')\,\mathrm{d}\mathbf{r}\,\mathrm{d}\mathbf{r}'\end{aligned} \tag{10.6.8}$$

where n_+, n_- are the number densities in the bulk.

The direct correlation functions in (10.6.8) may be decomposed in the form

$$c_{\nu\mu}(\mathbf{r}, \mathbf{r}') = c_{\nu\mu}^{\mathrm{S}}(\mathbf{r}, \mathbf{r}') - z_\nu z_\mu l_{\mathrm{B}}/|\mathbf{r}' - \mathbf{r}| \tag{10.6.9}$$

where $l_{\mathrm{B}} = e^2/\varepsilon k_{\mathrm{B}}T$ is called the Bjerrum length. The second term on the right-hand side is the asymptotic value of the function; the first term therefore represents the short-range correlations. If we now substitute for $c_{\nu\mu}(\mathbf{r}, \mathbf{r}')$ in (10.6.8), the excess free-energy functional separates into a mean-field, purely coulombic part, $\mathcal{F}^{\mathrm{C}}$, and a correlation term, $\mathcal{F}^{\mathrm{corr}}$. The mean-field part is given by (10.6.5), with $\mathcal{G}(\mathbf{r}, \mathbf{r}')$ taking its coulombic form, and the correlation term is formally identical to (10.6.8), but with the direct correlation functions replaced by their short-range parts. Thus

$$\mathcal{F}^{\mathrm{ex}} = \mathcal{F}^{\mathrm{C}} + \mathcal{F}^{\mathrm{corr}}, \quad \mathcal{F}^{\mathrm{C}} = \tfrac{1}{2}e^2 \iint \frac{\rho_Z(\mathbf{r})\rho_Z(\mathbf{r}')}{\varepsilon|\mathbf{r}' - \mathbf{r}|}\,\mathrm{d}\mathbf{r}\,\mathrm{d}\mathbf{r}' \tag{10.6.10}$$

A particularly simple approximation is to set $\mathcal{F}^{\mathrm{corr}} = 0$, implying that the fluid behaves as an ideal gas in which each ion experiences only the average electrostatic potential due to other ions and the charges at any interfaces. The density profile $\rho_\nu^{(1)}(\mathbf{r})$ derived from the variational principle (3.4.3) is then

$$\rho_\nu^{(1)}(\mathbf{r}) = \xi_\nu \exp\big(-\beta\big[\phi_\nu(\mathbf{r}) + z_\nu e\Phi^{\mathrm{C}}(\mathbf{r})\big]\big) \tag{10.6.11}$$

where the electrostatic potential $\Phi^{\mathrm{C}}(\mathbf{r})$ is given by (10.6.4) and $\xi_\nu = \exp(\beta\mu_\nu)/\Lambda_\nu^3$ is the activity of species ν, which in the mean-field approximation is equal to the bulk density n_ν.

If the external potentials have a coulombic component, arising from an external charge density $\rho_Z^{\text{ext}}(\mathbf{r})$, (10.6.11) may be rewritten as

$$\rho_\nu^{(1)}(\mathbf{r}) = n_\nu \exp\bigl(-\beta\bigl[\phi_\nu^{\text{S}}(\mathbf{r}) + z_\nu e\Phi(\mathbf{r})\bigr]\bigr) \tag{10.6.12}$$

where $\phi_\nu^{\text{S}}(\mathbf{r})$ is the short-range, non-coulombic contribution to $\phi_\nu(\mathbf{r})$ and $\Phi(\mathbf{r})$ is the total electrostatic potential, which is related to the total charge density by

$$\nabla^2\Phi(\mathbf{r}) = -\frac{4\pi e}{\varepsilon}\bigl[\rho_Z^{\text{ext}}(\mathbf{r}) + \rho_Z(\mathbf{r})\bigr] \tag{10.6.13}$$

The coupled equations (10.6.11) (or (10.6.12)) and (10.6.3) (or (10.6.13)) are the equations of Poisson–Boltzmann theory.

As a first application of the theory we take the case of an electric double layer near an inpenetrable, planar wall at $z = 0$. The wall separates the ionic solution for $z > 0$ from a dielectric medium of the same permittivity for $z < 0$; the density profiles now depend only on z. The wall carries a surface charge density σ and overall charge neutrality requires that

$$\int_0^\infty e\rho_Z(z)\,\mathrm{d}z = -\sigma \tag{10.6.14}$$

If we assume that the absolute charges of the two ionic species are equal, it follows that $n_+ = n_- = \frac{1}{2}n_0$, and combination of (10.6.2), (10.6.12) and (10.6.13) gives

$$\frac{\mathrm{d}^2\Phi(z)}{\mathrm{d}z^2} = \frac{4\pi e n_0}{\varepsilon}\sinh\bigl[\beta e\Phi(z)\bigr], \quad z > 0 \tag{10.6.15}$$

with the constraint, valid for point ions, that $\rho_\nu^{(1)}(z) = 0$ for $z < 0$. Equation (10.6.15) is the Poisson–Boltzmann equation; it must be solved subject to two boundary conditions:

$$\lim_{z\to 0}\frac{\mathrm{d}\Phi(z)}{\mathrm{d}z} = 0, \qquad \left.\frac{\mathrm{d}\Phi(z)}{\mathrm{d}z}\right|_{z=0} = -\frac{4\pi\sigma}{\varepsilon} \tag{10.6.16}$$

The local number density of microions is $\rho_N(z) = \rho_+^{(1)}(z) + \rho_-^{(1)}(z)$, the gradient of which is easily obtained from (10.6.2), (10.6.12) and (10.6.13):

$$\frac{\mathrm{d}\rho_N(z)}{\mathrm{d}z} = -\beta\frac{\mathrm{d}\Phi(z)}{\mathrm{d}z}e\rho_Z(z) = \frac{\beta\varepsilon}{4\pi}\frac{\mathrm{d}\Phi(z)}{\mathrm{d}z}\frac{\mathrm{d}^2\Phi(z)}{\mathrm{d}z^2} = \frac{\beta\varepsilon}{8\pi}\frac{\mathrm{d}}{\mathrm{d}z}\left(\frac{\mathrm{d}\Phi(z)}{\mathrm{d}z}\right)^2 \tag{10.6.17}$$

Integration of both sides of (10.6.17) from z to infinity yields a relation between the local number density and the local electric field $E(z) = -\mathrm{d}\Phi(z)/\mathrm{d}z$:

$$k_{\text{B}}T\bigl[\rho_N(z) - n_0\bigr] = \frac{\varepsilon}{8\pi}\bigl[E(z)\bigr]^2 \tag{10.6.18}$$

Since the microions behave as an ideal gas, the left-hand side of (10.6.18) is the difference in local osmotic pressure $P(z) = k_B T \rho_N(z)$ between a point z and a point in the bulk, where $\rho_N(z) = n_0$; the right-hand side is the electrostatic pressure,[28] which vanishes in the bulk. Differentiation of (10.6.18) with respect to z and use of Poisson's equation leads to the condition necessary for hydrostatic equilibrium, i.e.

$$\frac{\mathrm{d}P(z)}{\mathrm{d}z} = eE(z)\rho_Z(z) = f(z) \tag{10.6.19}$$

where $f(z)$ is the local force per unit volume acting on the solution. By evaluating (10.6.18) at $z = 0$ and making use of the second of the boundary conditions (10.6.16), we obtain an expression for the enhancement of the microion density at contact over its bulk value:

$$k_B T \rho_N(0) = k_B T n_0 + \frac{\varepsilon[E(0)]^2}{8\pi} = k_B T n_0 + \frac{2\pi\sigma^2}{\varepsilon} \tag{10.6.20}$$

This result is a special case of the contact theorem for ionic systems:[31]

$$k_B T \rho_N(0) = P + \frac{2\pi\sigma^2}{\varepsilon} \tag{10.6.21}$$

where P is the bulk osmotic pressure, which for an ideal solution is equal to $k_B T n_0$. Equation (10.6.21) is a generalisation of (6.5.3b), which applies to uncharged systems. As the surface charge increases, the contact density will eventually become sufficiently large that the role of ion–ion correlations can no longer be ignored. The correlation term in the free-energy functional (10.6.10) must then be included in some approximate form,[32] such as a weighted-density approximation of the type discussed in Section 6.2.

Equation (10.6.15) can be solved analytically. The dimensionless potential $\Phi^*(z) = e\Phi(z)/k_B T$ satisfies the equation

$$\frac{\mathrm{d}^2\Phi^*(z)}{\mathrm{d}z^2} = k_D^2 \sinh \Phi^*(z) \tag{10.6.22}$$

where k_D is the Debye wavenumber (10.2.15). The solution to (10.6.22) is

$$\Phi^*(z) = 4\tanh^{-1}\left[g \exp(-k_D z)\right] \tag{10.6.23}$$

where g is related to the dimensionless surface potential $\Phi^*(0)$ by

$$g = \tanh \tfrac{1}{4}\Phi^*(0) \tag{10.6.24}$$

The density profiles follow from (10.6.11):

$$\rho_{\pm}^{(1)}(z) = \tfrac{1}{2} n_0 \left(\frac{1 \mp g \exp(-k_D z)}{1 \pm g \exp(-k_D z)} \right)^2 \tag{10.6.25}$$

At distances $z \approx k_{\mathrm{D}}^{-1}$ or larger, the density profiles approach their bulk values exponentially, so the thickness of the double layer is of the order of Λ_{D}, the Debye screening length.

We next consider the question of what the effective interaction is between charged surfaces separated by an inhomogeneous ionic solution. The simplest geometry is that of two infinite, parallel, uniformly charged planes placed at $z = \pm\frac{1}{2}L$. If the two surface charge densities are the same, there is a plane of symmetry at $z = 0$ where the local electric field must vanish. The ionic fluid is assumed to be in chemical equilibrium with a reservoir of non-interacting, monovalent microions, which fixes the chemical potentials of the two species at their ideal values, $\mu_\nu = k_{\mathrm{B}}T \ln(\Lambda_\nu^3 n_\nu)$. The mirror symmetry means that it is necessary to solve the Poisson–Boltzmann equation only in the interval $-\frac{1}{2}L \leqslant z \leqslant 0$, with the boundary conditions

$$\left.\frac{\mathrm{d}\Phi(z)}{\mathrm{d}z}\right|_{z=-L/2} = -\frac{4\pi\sigma}{\varepsilon}, \qquad \left.\frac{\mathrm{d}\Phi(z)}{\mathrm{d}z}\right|_{z=0} = 0 \tag{10.6.26}$$

For this problem, apart from the somewhat academic case when the solution contains only counterions, the solution to the non-linear differential equation (10.6.15) must be obtained numerically. If the surface charge σ is sufficiently low, however, it is justifiable to linearise (10.6.22) by setting $\sinh\Phi^*(z) \approx \Phi^*(z)$. The resulting linear equation is easily solved to give

$$\Phi(z) = \frac{\Phi_0}{\sinh(k_{\mathrm{D}}L/2)}\cosh(k_{\mathrm{D}}z) \tag{10.6.27}$$

with $\Phi_0 = 4\pi\sigma/\varepsilon k_{\mathrm{D}}$.

The normal component $P_{\mathrm{N}}(z)$ of the stress tensor determines the force per unit area on a test surface placed at z within the fluid. In mechanical equilibrium, P_{N} must be constant throughout the interval between the planes, i.e.

$$\frac{\mathrm{d}P_{\mathrm{N}}(z)}{\mathrm{d}z} = 0, \quad -\tfrac{1}{2}L < z < \tfrac{1}{2}L \tag{10.6.28}$$

The quantity $P_{\mathrm{N}}(z)$ is the sum of the osmotic pressure of the ions, $P(z) = k_{\mathrm{B}}T\rho_N(z)$, and an electrostatic contribution, which is related to Maxwell's electrostatic stress tensor:[28]

$$P_{\mathrm{N}} = P(z) - \frac{\varepsilon}{8\pi}\left(\frac{\mathrm{d}\Phi(z)}{\mathrm{d}z}\right)^2 = k_{\mathrm{B}}T\rho_N(z) - \frac{\varepsilon}{8\pi}\big[E(z)\big]^2 \tag{10.6.29}$$

Taken together, (10.6.28) and (10.6.29) lead back to the equilibrium condition (10.6.19). The pressure difference

$$\Delta P = P_{\mathrm{N}}(L) - P_{\mathrm{N}}(\infty) \tag{10.6.30}$$

is the force per unit area that must be applied to the charged planes in order to maintain them at a separation L; it can therefore be identified with the solvation force f_{S} introduced in Section 6.1. Since the local electrical field is zero at $z = 0$, it follows from (10.6.29) that

$$f_{\mathrm{S}} \equiv \Delta P = k_{\mathrm{B}}T\big[\rho_N(0) - n_0\big] \tag{10.6.31}$$

Combination of (10.6.27), (10.6.31) and the linearised version of (10.6.12) shows that to lowest, non-vanishing order in $\Phi(z=0)$:

$$f_{\mathrm{S}}(L) = \tfrac{1}{2}k_{\mathrm{B}}Tn_0\big[\beta e\Phi(0)\big]^2 = \frac{2\pi\sigma^2}{\varepsilon}\frac{1}{\sinh^2(k_{\mathrm{D}}L/2)}$$
$$\approx \frac{8\pi\sigma^2}{\varepsilon}\exp(-k_{\mathrm{D}}L) \tag{10.6.32}$$

Thus the effective interaction between the charged plates is always repulsive. The same conclusion is reached within non-linear Poisson–Boltzmann theory. However, when correlations between ions are taken into account, the force between the planes may become attractive at small separations.[33] Such correlations are particularly strong in the case of divalent (or polyvalent) counterions, as illustrated by the results of Monte Carlo calculations shown in Figure 10.6.

Attraction between two like-charged surfaces can be accounted for within density-functional theory only if the correlation term in the excess free-energy functional is adequately approximated. If the ions are modelled as charged hard spheres, the correlations between ions arise both from hard-core effects and from short-range, coulombic interactions. This suggests that $\mathcal{F}^{\mathrm{ex}}$ can be usefully rewritten as

$$\mathcal{F}^{\mathrm{ex}}\big[\rho_+^{(1)}, \rho_-^{(1)}\big]$$
$$= \tfrac{1}{2}\int e\rho_Z(\mathbf{r})\Phi(\mathbf{r})\,\mathrm{d}\mathbf{r} + \mathcal{F}^{\mathrm{HS}}\big[\rho_+^{(1)}, \rho_-^{(1)}\big]$$
$$- k_{\mathrm{B}}T\sum_{\nu}\sum_{\mu}\int_0^1 \mathrm{d}\lambda(1-\lambda)\iint \Delta\rho_\nu^{(1)}(\mathbf{r})\Delta c_{\nu\mu}(\mathbf{r},\mathbf{r}';\lambda)\Delta\rho_\mu^{(1)}(\mathbf{r}')\,\mathrm{d}\mathbf{r}\,\mathrm{d}\mathbf{r}' \tag{10.6.33}$$

The first term on the right-hand side of (10.6.33) is the mean-field, purely coulombic contribution; the second is the excess free-energy functional for a binary hard-sphere mixture, corresponding to uncharged ions; and the last term contains the "residual" direct correlation functions, defined as

$$\Delta c_{\nu\mu}(\mathbf{r},\mathbf{r}';\lambda) = c_{\nu\mu}(\mathbf{r},\mathbf{r}';\lambda) + \frac{z_\nu z_\mu \lambda l_{\mathrm{B}}}{|\mathbf{r}-\mathbf{r}'|} - c_{\nu\mu}^{\mathrm{HS}}(\mathbf{r},\mathbf{r}';\lambda) \tag{10.6.34}$$

and represents the remaining correlations.[34] The hard-sphere direct correlation functions $c_{\nu\mu}^{\mathrm{HS}}(\mathbf{r}'\mathbf{r}')$ are those compatible with the assumed form of the functional $\mathcal{F}^{\mathrm{HS}}$, for which a weighted-density approximation can be used, and the residual direct correlation functions can be replaced by those of the bulk solution obtained, for example, from the solution of the MSA given in Section 10.3. Figure 10.6 makes a comparison between the results obtained in this way and those of Poisson–Boltzmann theory for restricted primitive models of both 1 : 1 and 2 : 2 electrolyte solutions. In the case of the 1 : 1 solution, where the force is everywhere repulsive, the two theories give similar results. In the divalent system, however, the inclusion of correlations gives rise to a strongly attractive force at small separations, with a minimum at $L \approx 2d$; the results are in good agreement with those obtained by

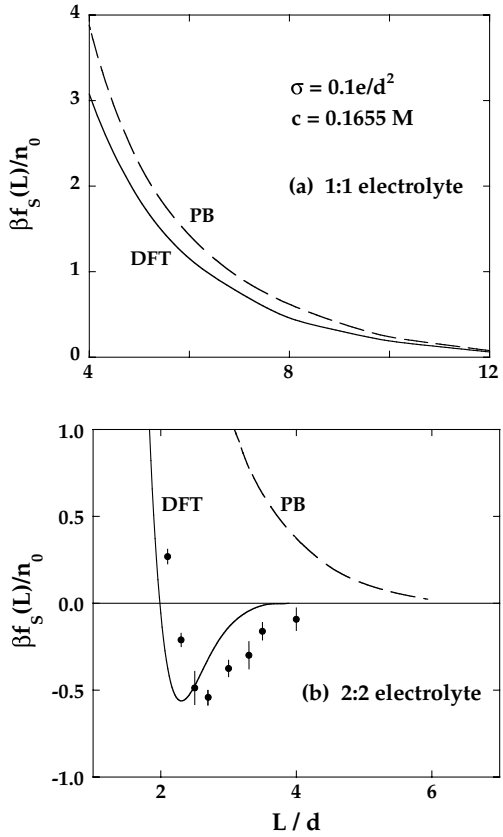

FIG. 10.6. Electric double-layer force between charged plates in restricted primitive models of (a) 1 : 1 and (b) 2 : 2 electrolyte solutions as a function of the plate separation L. The state conditions correspond in each case to an aqueous solution of ions of diameter $d = 4.2$ Å at 298 K. The curves are calculated from the Poisson–Boltzmann approximation (PB) or from density-functional theory (DFT) and the points are the results of Monte Carlo simulations.[33(b)] See text for details. After Tang *et al.*[34]

simulation for the same system. Poisson–Boltzmann theory, by contrast, again predicts that the force should be repulsive for all L. Ion correlations may also lead to charge inversion or "overscreening" of the surface charge: the total charge of the double layer, integrated over a few ionic diameters, can be of opposite sign to that of the planes. Similar results have been reached on the basis of numerical solution of the so-called anisotropic HNC equation, which represents an extension of bulk HNC theory to inhomogeneous situations.[35]

10.7 EFFECTIVE INTERACTIONS BETWEEN COLLOIDAL PARTICLES

We now show how the methods developed in the previous section can be used to calculate the effective interaction between large polyions in solution. The example we choose

is that of a dispersion of spherical, colloidal particles in a polar solvent of dielectric constant ε. The radius R of a particle, which we treat as a hard sphere, would be typically tens or even hundreds of nanometres, and the particle would carry a charge Ze ($|Z| \gg 1$), with the consequent formation of an electric double layer at the surface. We again adopt a primitive-model description of the solvent, with both coions and counterions being represented as charged hard spheres of diameter d ($\ll R$), and assume that the dispersion is in equilibrium with a salt reservoir, which fixes the chemical potentials μ_+, μ_- of the microions. The three-component system can be described within the so-called semi-grand canonical ensemble, characterised by the variables N_0, μ_+, μ_-, V and T, in which the number of polyions, N_0, is fixed but the numbers of microions are allowed to fluctuate. If we denote the coordinates of the polyions and microions by $\{\mathbf{R}_i\}$ and $\{\mathbf{r}_j\}$, respectively, the total potential energy of the system may be written in a shorthand form in which subscripts 0 and M refer, respectively, to polyions and microions:

$$V\big(\{\mathbf{R}_i\},\{\mathbf{r}_j\}\big) = V_{00}\big(\{\mathbf{R}_i\}\big) + V_{0\mathrm{M}}\big(\{\mathbf{R}_i\},\{\mathbf{r}_j\}\big) + V_{\mathrm{MM}}\big(\{\mathbf{r}_j\}\big) \tag{10.7.1}$$

where V_{00}, $V_{0\mathrm{M}}$ and V_{MM} are all sums of pair potentials of primitive-model form.

The large difference, both in size and charge, between polyions and microions renders the conventional integral-equation approaches impractical. A coarse-graining strategy is needed whereby the degrees of freedom of the microions are averaged out, so reducing the problem to that of an effective, one-component system of polyions dressed by their electric double layers. The reduction is achieved by writing the partition function of the semi-grand canonical system in the form

$$Q_{N_0} = \frac{1}{N_0!\Lambda_0^{3N_0}} \int \exp(-\beta V_{00})\,\Xi_{\mathrm{M}}\big(\mu_+,\mu_-,V,T;\{\mathbf{R}_i\}\big)\,\mathrm{d}\mathbf{R}^{N_0} \tag{10.7.2}$$

where

$$\Xi_{\mathrm{M}} = \sum_{N_+=0}^{\infty}\sum_{N_-=0}^{\infty} \frac{\xi_+^{N_+}\xi_-^{N_-}}{N_+!N_-!} \iint \exp\big[-\beta(V_{0\mathrm{M}}+V_{\mathrm{MM}})\big]\,\mathrm{d}\mathbf{r}^{N_+}\,\mathrm{d}\mathbf{r}^{N_-} \tag{10.7.3}$$

is the grand partition function of the microions in the external potential $\phi_\nu(\mathbf{r})$ of the polyions in a configuration $\{\mathbf{R}_i\}$:

$$\phi_\nu(\mathbf{r}) = \sum_{i=1}^{N_0} v_{0\nu}\big(|\mathbf{r}-\mathbf{R}_i|\big) \tag{10.7.4}$$

and ξ_+, ξ_- are the activities of the microions. Equation (10.7.2) can be re-expressed as

$$Q_{N_0} = \frac{1}{N_0!\Lambda_0^{3N_0}} \int \exp\big(-\beta V_{\mathrm{eff}}\big(\{\mathbf{R}_i\}\big)\big)\,\mathrm{d}\mathbf{R}^{N_0} \tag{10.7.5}$$

in which the effective interaction between the dressed polyions is

$$V_{\text{eff}}\big(\{\mathbf{R}_i\}\big) = V_{00}\big(\{\mathbf{R}_i\}\big) + \Omega_{\text{M}}\big(\mu_+, \mu_-, V, T; \{\mathbf{R}_i\}\big) \tag{10.7.6}$$

where $\Omega_{\text{M}} = -k_{\text{B}}T \ln \Xi_{\text{M}}$ is the grand potential of the microions. The first term on the right-hand side of (10.7.6) arises from the direct interaction between polyions, while the second is a state-dependent, microion-induced interaction, which depends parametrically on the coordinates $\{\mathbf{R}_i\}$. Whereas the direct interaction is pairwise additive, the effective interaction is not; the effective interaction also includes a "volume" term, which is independent of the polyion coordinates.

The grand potential Ω_{M} can be evaluated by the methods of density-functional theory. If we limit ourselves to a mean-field approach, we can take over the grand-potential functional defined by (10.6.6), (10.7.7) and (10.6.10) (with $\mathcal{F}^{\text{corr}} = 0$). The solution of the resulting Euler–Lagrange equations for the local densities $\rho_\nu^{(1)}(\mathbf{r})$ in the multi-centre external potential (10.7.4) poses a formidable task. Numerical results may be obtained through a form of molecular-dynamics calculation in which the Fourier components of the local densities are treated as dynamical variables,[36] a scheme inspired by the Car–Parrinello method for simulating systems of classical ions and quantum mechanical, valence electrons.[37] However, further progress can be made analytically if the inhomogeneities induced by the polyions are assumed to be weak. In that case it is justifiable to expand the ideal free-energy functional (3.1.22) to second order in the deviation $\Delta\rho_\nu^{(1)}(\mathbf{r})$ of the local density from its bulk value, i.e.

$$\Delta\rho_\nu^{(1)}(\mathbf{r}) = \rho_\nu^{(1)}(\mathbf{r}) - n_\nu \tag{10.7.7}$$

The intrinsic free-energy functional of the microions is then

$$\mathcal{F}\big[\rho_+^{(1)}, \rho_-^{(1)}\big] = \sum_\nu \Bigg(F^{\text{id}}(n_\nu) + k_{\text{B}}T \ln\big(\Lambda_\nu^3 n_\nu\big) \int \Delta\rho_\nu^{(1)}(\mathbf{r})\, \mathrm{d}\mathbf{r} + \frac{k_{\text{B}}T}{2n_\nu} \int \big[\Delta\rho_\nu^{(1)}\mathbf{r}\big]^2 \, \mathrm{d}\mathbf{r} \Bigg) + \tfrac{1}{2} \int e\rho_Z(\mathbf{r}) \Phi^{\text{C}}(\mathbf{r})\, \mathrm{d}\mathbf{r} \tag{10.7.8}$$

where the electrostatic potential $\Phi^{\text{C}}(\mathbf{r})$ satisfies Poisson's equation (10.6.3). Substitution of (10.7.8) in (10.6.6), replacement of the chemical potentials μ_ν by their ideal values and use of the variational principle (3.4.3) gives

$$\frac{\Delta\rho_\nu^{(1)}(\mathbf{r})}{n_\nu} + z_\nu \Phi^{\text{C}}(\mathbf{r}) = -\beta\phi_\nu(\mathbf{r}), \quad \nu = +, - \tag{10.7.9}$$

These two equations are coupled through the terms in Φ^{C}. If we were to suppose for the moment that the polyions are point particles, i.e. that $R = 0$, the coulombic contribution to $\phi_\nu(\mathbf{r})$ would be everywhere equal to $z_\nu e \Phi^{\text{ext}}(\mathbf{r})$, where $\Phi^{\text{ext}}(\mathbf{r})$ is the "external" electrostatic potential acting on the microions.[38] If there were no boundaries, the total electrostatic

potential within the fluid would then be

$$\Phi(\mathbf{r}) = \Phi^{\mathrm{C}}(\mathbf{r}) + \Phi^{\mathrm{ext}}(\mathbf{r}) = e\int \frac{\rho_Z(\mathbf{r}') + Z\rho^{\mathrm{ext}}(\mathbf{r}')}{\varepsilon|\mathbf{r}-\mathbf{r}'|}\,\mathrm{d}\mathbf{r}' \tag{10.7.10}$$

where $\rho^{\mathrm{ext}}(\mathbf{r}) = \sum_i \delta(\mathbf{r}-\mathbf{R}_i)$ is the microscopic density of the polyions. Equation (10.7.9) now becomes

$$\Delta\rho_\nu^{(1)}(\mathbf{r}) = -\frac{n_\nu z_\nu e^2}{k_{\mathrm{B}}T}\int \frac{\rho_Z(\mathbf{r}') + Z\rho^{\mathrm{ext}}(\mathbf{r}')}{\varepsilon|\mathbf{r}-\mathbf{r}'|}\,\mathrm{d}\mathbf{r}' \tag{10.7.11}$$

To simplify the problem, we consider only the salt-free case, where all microions are counterions. The coupled equations (10.7.11) then reduce to a single integral equation from which the subscript ν can be dropped and the charge density $\rho_Z(\mathbf{r})$ replaced by $z\rho^{(1)}(\mathbf{r})$. On taking Fourier transforms of both sides of (10.7.11), applying the convolution theorem and incorporating the result in (10.1.5), we find that the Fourier transform of $\Delta\rho^{(1)}(\mathbf{r})$ is

$$\hat{\rho}^{(1)}(\mathbf{k}) = \frac{Zk_{\mathrm{D}}^2}{k^2+k_{\mathrm{D}}^2}\sum_{i=1}^{N_0}\exp(-i\mathbf{k}\cdot\mathbf{R}_i) \tag{10.7.12}$$

where $k_{\mathrm{D}}^2 = 4\pi n z^2 e^2/\varepsilon k_{\mathrm{B}}T$ is the square of the Debye wavenumber associated with the counterions. Inverse Fourier transformation of (10.7.12) leads to a counterion density profile given by

$$\rho^{(1)}(\mathbf{r}) = \sum_{i=1}^{N_0}\frac{Zk_{\mathrm{D}}^2}{4\pi}\frac{\exp(-k_{\mathrm{D}}|\mathbf{r}-\mathbf{R}_i|)}{|\mathbf{r}-\mathbf{R}_i|} \equiv \sum_{i=1}^{N_0}\rho_i^{(1)}(\mathbf{r}) \tag{10.7.13}$$

The total profile is therefore a superposition of profiles associated with each of the polyions. The radius of the polyions is now reintroduced by imposing the constraint that $\rho_i^{(1)}(\mathbf{r})$ must be zero whenever $|\mathbf{r}-\mathbf{R}_i| < R$. Charge neutrality means that $\rho_i^{(1)}(\mathbf{r})$ must be normalised such that

$$\int_{|\mathbf{r}-\mathbf{R}_i|>R}\rho_i^{(1)}(\mathbf{r})\,\mathrm{d}\mathbf{r} = |Z/z| \tag{10.7.14}$$

and for the profile defined by (10.7.13) this requirement would be met if the polyion charge Ze were replaced by a renormalised charge $Z'e$, where

$$Z' = Z\frac{\exp(k_{\mathrm{D}}R)}{1+k_{\mathrm{D}}R} \tag{10.7.15}$$

The normalisation in (10.7.14) implicitly assumes that the colloid concentration is low and hence that the electric double-layers associated with neighbouring polyions have, on average, little overlap. From Poisson's equation it is evident that the total electrostatic

potential may similarly be written as a superposition of N_0 screened potentials:

$$\Phi(\mathbf{r}) = \sum_{i=1}^{N_0} \frac{Z'e}{\varepsilon} \frac{\exp(-k_{\mathrm{D}}|\mathbf{r}-\mathbf{R}_i|)}{|\mathbf{r}-\mathbf{R}_i|} \equiv \sum_{i=1}^{N_0} \Phi_i(\mathbf{r}) \tag{10.7.16}$$

If the density profile (10.7.13) and the potential (10.7.16) are substituted in the free-energy functional (10.7.8), we find that the effective interaction energy (10.7.6) is of the form

$$V_{\mathrm{eff}}\big(\{\mathbf{R}_i\}\big) = V_0 + \sum_{i=1}^{N} \sum_{j>i}^{N} v_{\mathrm{eff}}\big(|\mathbf{R}_i - \mathbf{R}_j|\big) \tag{10.7.17}$$

where the effective pair potential $v_{\mathrm{eff}}(R)$ provides the electrostatic contribution to the well-known Derjaguin–Landau–Verwey–Overbeek (DLVO) potential:[39]

$$\begin{aligned} v_{\mathrm{eff}}\big(|\mathbf{R}_i - \mathbf{R}_j|\big) &= \int \Phi_i(\mathbf{r}) \rho_j^{(1)}(\mathbf{r})\, \mathrm{d}\mathbf{r} \\ &= \frac{Z'^2 e^2}{\varepsilon} \frac{\exp(-k_{\mathrm{D}}|\mathbf{R}_i - \mathbf{R}_j|)}{|\mathbf{R}_i - \mathbf{R}_j|} \end{aligned} \tag{10.7.18}$$

The pairwise additivity is a consequence of the quadratic form of the approximate functional (10.7.8).

The effective interaction energy (10.7.17) contains a structure-independent term, V_0. This term has no effect on the forces acting between the polyions, but it has a significant influence on the phase diagram.[40] It includes, among other contributions, the self-energy of the double layers associated with individual polyions. The DLVO potential is a function of density and temperature through its dependence on the Debye wavenumber; its form remains the same even in the presence of coions, provided the contributions of all microions are included in the definition of k_{D} and in V_0. It is strictly repulsive, thereby stabilising the colloidal suspension against irreversible aggregation (flocculation) induced by the strong van der Waals attractive forces between particles. However, if the salt concentration is sufficiently low, the structure-independent term can drive a phase transition into colloid-rich and colloid-poor dispersions, even in the absence of attractive forces.

The quadratic functional is inadequate for highly-charged polyions. The strong electrostatic attraction exerted by the polyions on the counterions leads to a substantial fraction of the latter becoming tightly bound to the colloid surface; this reduces[41] the magnitude of the bare polyion charge to an effective value $|Z_{\mathrm{eff}}|e$. The remaining counterions therefore experience a much weaker external potential, so the diffuse part of the double layer can still be described within the quadratic approximation. Direct measurement of the effective pair potential between charged colloidal particles shows that (10.7.18) provides a good representation of the data when Z_{eff} is suitably chosen, as the results shown in Figure 10.7 illustrate. The strong, coulombic correlations between microions that arise in the presence of divalent or trivalent counterions lead to a short-range attraction between like-charged polyions, similar to that calculated for planar surfaces in Section 10.6.

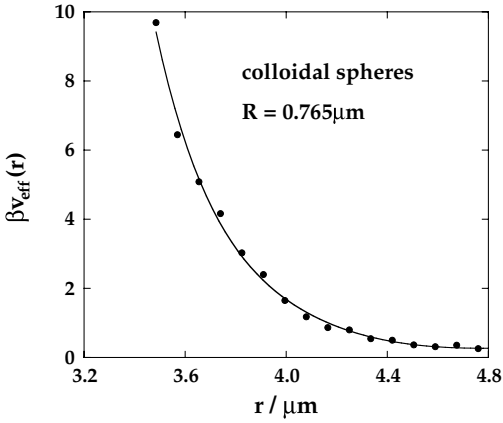

FIG. 10.7. Effective pair potential between polystyrene sulphate spheres of radius 0.765 ± 0.01 μm dispersed in water. The points are experimental results and the curve is calculated from (10.7.18) for an effective charge $|Z_{\text{eff}}| = 22\,793$. After Crocker and Grier.[42]

10.8 LIQUID METALS: ELECTRONS AND IONS

Pure liquid metals are two-component fluids consisting of N_{i} positive ions and $N_{\text{e}} = zN_{\text{i}}$ conduction electrons, where z is the ionic valency. The ionic core radius is usually only a small fraction of the mean interionic spacing, with the result that the ion cores occupy less than 10% of the total volume of the metal. In the "nearly free electron" picture the conduction electrons are assumed to move more or less freely through the liquid, interacting only rarely with the ions; the mean-free path of the electrons is typically ten to a hundred times larger than the separation of neighbouring ions. In the crudest approximation, interactions are neglected altogether, and the electrons are treated as an ideal Fermi gas characterised by the energy ε_{F} of the highest occupied (Fermi) level, i.e. $\varepsilon_{\text{F}} = \hbar^2 k_{\text{F}}^2/2m_{\text{e}} = \hbar^2(3\pi^2\rho_{\text{e}})^{2/3}/2m_{\text{e}}$, where k_{F} is the Fermi wavenumber, ρ_{e} is the number density of conduction electrons and m_{e} is the electron mass. The Fermi temperature, $T_{\text{F}} = \varepsilon_{\text{F}}/k_{\text{B}}$, is always some two orders of magnitude higher than the melting temperature. It is therefore a good approximation to assume that the electron gas is completely degenerate under normal liquid–metal conditions.

The simplest model that takes account of electron–ion interactions is the "jellium" model of Wigner. This is the quantum-mechanical analogue of the one-component plasma (OCP) discussed in Section 10.1. It treats the conduction electrons as an interacting Coulomb gas moving in the uniform background provided by the positively charged ions, with a hamiltonian $\mathcal{H} = K_{N_{\text{e}}} + V_{N_{\text{e}}}$, where $K_{N_{\text{e}}}$ is the kinetic-energy operator and the potential energy $V_{N_{\text{e}}}$ is the sum of electron–electron, electron–background and background–background terms. In a **k**-space representation, $V_{N_{\text{e}}}$ is given as a special case of (10.1.4) by

$$V_{N_{\text{e}}} = \frac{1}{2V}{\sum_{\mathbf{k}}}' \hat{v}_{\text{ee}}(k)\left(\rho^{\text{e}}_{\mathbf{k}}\rho^{\text{e}}_{-\mathbf{k}} - N_{\text{e}}\right) \tag{10.8.1}$$

where $\rho^{\mathrm{e}}_{\mathbf{k}}$ is a Fourier component of the microscopic electron density, $\hat{v}_{\mathrm{ee}}(k) = 4\pi e^2/k^2$ is the Fourier transform of the electron–electron potential and the prime on the summation means that the contribution for $\mathbf{k} = 0$ is omitted because of cancellation by the background. The ground-state energy has been calculated by methods of quantum-mechanical many-body theory;[43] it is the sum of kinetic, exchange and correlation terms and is expressible as a function of the single, dimensionless parameter $r_{\mathrm{S}} = a_{\mathrm{e}}/a_0$, where $a_{\mathrm{e}} = (3/4\pi\rho_{\mathrm{e}})^{1/3}$ is the "electron-sphere" radius and a_0 is the Bohr radius. The minimum energy, corresponding to zero pressure, occurs at $r_{\mathrm{S}} \approx 4.2$. This result is independent of the chemical nature of the system, but is in fair agreement with experimental results for the alkali metals, which range from 3.30 (for Li) to 5.78 (for Cs).

In a more realistic model the hamiltonian of a liquid metal is written as the sum of a purely electronic term $\mathcal{H}_{\mathrm{e}}$, a purely ionic term $\mathcal{H}_{\mathrm{i}}$ and an electron–ion interaction V_{ei}. The Coulomb repulsion between ions is in general sufficiently strong to prevent any short-range forces coming into play, while dispersion forces are weak because the ion cores are only weakly polarisable. It is therefore a good approximation to set the ion–ion interaction $v_{\mathrm{ii}}(R)$ equal to z^2e^2/R for all R. The electron–electron interaction $v_{\mathrm{ee}}(r)$ is purely coulombic and the electron–ion potential v_{ei} is also coulombic outside the ion core; we shall see below that inside the core, v_{ei} can be replaced by a weak "pseudopotential". We proceed[44] by adding to and subtracting from the hamiltonian the two contributions that would arise if the electrons were replaced by a uniform background of charge density $-e\rho_{\mathrm{e}}$. The terms involved are the ion–background interaction V_{ib} and the background self-energy V_{bb}, given by

$$V_{\mathrm{ib}} = -\rho_{\mathrm{e}} \sum_{j=1}^{N_{\mathrm{i}}} \int \frac{ze^2}{|\mathbf{R}_j - \mathbf{r}|}\,\mathrm{d}\mathbf{r}, \qquad V_{\mathrm{bb}} = \tfrac{1}{2}\rho_{\mathrm{e}}^2 \iint \frac{e^2}{|\mathbf{r} - \mathbf{r}'|}\,\mathrm{d}\mathbf{r}\,\mathrm{d}\mathbf{r}' \tag{10.8.2}$$

where $\mathbf{R}_j$ denotes the coordinates of ion j. The hamiltonian can then be written as

$$\mathcal{H} = \mathcal{H}'_{\mathrm{e}} + \mathcal{H}'_{\mathrm{i}} + V'_{\mathrm{ei}} \tag{10.8.3}$$

with

$$\mathcal{H}'_{\mathrm{e}} = \mathcal{H}_{\mathrm{e}} - V_{\mathrm{bb}}, \qquad \mathcal{H}'_{\mathrm{i}} = \mathcal{H}_{\mathrm{i}} + V_{\mathrm{ib}} + V_{\mathrm{bb}}, \qquad V'_{\mathrm{ei}} = V_{\mathrm{ei}} - V_{\mathrm{ib}} \tag{10.8.4}$$

In $\mathbf{k}$-space:

$$\begin{aligned}
\mathcal{H}'_{\mathrm{e}} &= K_{\mathrm{e}} + \frac{1}{2V}{\sum_{\mathbf{k}}}' \frac{4\pi e^2}{k^2}\left(\rho^{\mathrm{e}}_{\mathbf{k}}\rho^{\mathrm{e}}_{-\mathbf{k}} - N_{\mathrm{e}}\right) \\
\mathcal{H}'_{\mathrm{i}} &= K_{\mathrm{i}} + \frac{1}{2V}{\sum_{\mathbf{k}}}' \frac{4\pi z^2e^2}{k^2}\left(\rho^{\mathrm{i}}_{\mathbf{k}}\rho^{\mathrm{i}}_{-\mathbf{k}} - N_{\mathrm{i}}\right) \\
V'_{\mathrm{ei}} &= U_0 + \frac{1}{V}{\sum_{\mathbf{k}}}' \hat{v}_{\mathrm{ei}}(k)\rho^{\mathrm{i}}_{\mathbf{k}}\rho^{\mathrm{e}}_{-\mathbf{k}}
\end{aligned} \tag{10.8.5}$$

where K_i is the kinetic energy of the ions and

$$U_0 = \frac{1}{V}\lim_{k\to 0}\left(\hat{v}_{ei}(k) + \frac{4\pi z e^2}{k^2}\right)\rho^i_{\mathbf{k}}\rho^e_{-\mathbf{k}} = N_i\rho_e\int\left(v_{ei}(r) + \frac{ze^2}{r}\right)d\mathbf{r} \tag{10.8.6}$$

The term $\mathcal{H}'_e$ is the jellium hamiltonian and $\mathcal{H}'_i$ is the hamiltonian of an OCP of positive ions in a uniform background. In this formulation of the problem a liquid metal emerges as a "mixture" of a classical OCP and a quantum-mechanical jellium, the two components being coupled together through the term V'_{ei}.

Inside the ion core the interaction of the conduction electrons with the ion is determined by details of the charge distribution of the core electrons. The true electron–ion interaction is therefore a complicated, non-local function for $r < r_C$, where r_C is the ion-core radius. In addition, the potential has a singularity at $r = 0$. Despite these difficulties it is possible to treat the electron–ion coupling by perturbation theory if the interaction is recast in pseudopotential form. The procedure adopted in practice is to parametrise an assumed functional form for the pseudopotential by fitting to experimental results for quantities that are sensitive to electron–ion collisions. A particularly simple and widely adopted pseudopotential $v^*_{ei}(r)$ consists in taking

$$\begin{aligned} v^*_{ei}(r) &= 0, \qquad r < r_C, \\ &= -ze^2/r, \quad r > r_C \end{aligned} \tag{10.8.7}$$

This is called the "empty-core" pseudopotential;[45] values of the parameter r_C can be derived from transport and Fermi-surface data and lie close to generally accepted values for the ionic radii of simple metals.

If the pseudopotential is weak, the electron–ion term in (10.8.5) can be treated as a perturbation, the reference system being a superposition of a classical OCP and a degenerate, interacting electron gas. To lowest order in perturbation theory, the structure of each component of the reference system is unaffected by the presence of the other. In this approximation, assuming the two fluids to be homogeneous:

$$\langle\rho^i_{\mathbf{k}}\rho^e_{-\mathbf{k}}\rangle = \langle\rho^i_{\mathbf{k}}\rangle\langle\rho^e_{-\mathbf{k}}\rangle = 0, \quad \mathbf{k}\neq 0 \tag{10.8.8}$$

Hence, on averaging the perturbation V'_{ei}, only the structure-independent term survives. The internal energy of the metal is then the sum of three terms: the energy of the degenerate electron gas, given by the jellium model; the internal energy of the classical OCP, which is known from Monte Carlo calculations[46] as a function of the dimensionless coupling constant $\Gamma = z^2e^2/a_i k_B T$, where $a_i = (3/4\pi\rho_i)^{1/3}$; and the quantity U_0, which can be calculated from (10.8.6) and (10.8.7). When combined, these results allow the calculation of the internal energy and equation of state as functions of the density parameter r_S for values of Γ and r_C appropriate to a particular metal. Figure 10.8 shows the equation of state obtained in this way for four alkali metals along isotherms corresponding to the experimental melting temperatures. Given the crudeness of the model, the agreement between theory and experiment for the zero-pressure value of r_S is surprisingly good.

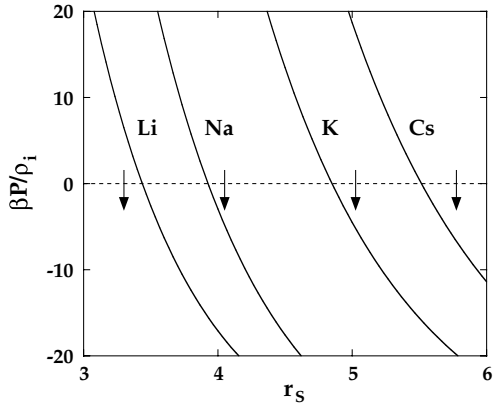

FIG. 10.8. Equation of state of four alkali metals along isotherms corresponding to the experimental melting temperatures (Li, 452 K; Na, 371 K; K, 337 K; Cs, 303 K). The curves are calculated from the first-order perturbation theory described in the text and the arrows mark the experimental values of r_S at atmospheric pressure.

A more accurate calculation has to take account of the influence of the ionic component on the structure of the electron gas and vice versa. To do so, we must go to second order in perturbation theory. We also use an adiabatic approximation: the electrons are assumed to adjust themselves instantaneously to the much slower changes in the ionic coordinates. Thus the problem to be considered is that of an inhomogeneous, interacting electron gas in the external field produced by a given ionic charge distribution; because the electron–ion pseudopotential is assumed to be weak, the influence of the external field can be treated by linear-response theory. The polarisation of the electron gas by the ionic charge distribution leads to a screening of the external field and hence, as we shall see, to a new, effective interaction between the ions. Although different in detail, the calculation is similar in spirit to that of the effective interaction between colloidal particles in solution, described in the previous section.

The partition function corresponding to the hamiltonian (10.8.3) is

$$Q_{N_\mathrm{i}N_\mathrm{e}} = \frac{1}{N_\mathrm{i}!h^{3N_\mathrm{i}}} \iint \exp(-\beta\mathcal{H}'_\mathrm{i}) \operatorname{Tr}_\mathrm{e} \exp\bigl[-\beta(\mathcal{H}'_\mathrm{e} + V'_\mathrm{ei})\bigr] \mathrm{d}\mathbf{R}^{N_\mathrm{i}} \, \mathrm{d}\mathbf{P}^{N_\mathrm{i}} \tag{10.8.9}$$

where $\mathbf{P}^{N_\mathrm{i}} \equiv \{\mathbf{P}_j\}$ represents the momenta of the ions. The trace is taken over a complete set of quantum states of the electron gas in the field due to a fixed ionic configuration; the free energy F'_e of the inhomogeneous electron gas is a function of the ionic coordinates $\{\mathbf{R}_j\}$ and given by

$$F'_\mathrm{e}\bigl(\{\mathbf{R}_j\}\bigr) = -k_\mathrm{B}T \ln\bigl(\operatorname{Tr}_\mathrm{e} \exp\bigl[-\beta(\mathcal{H}'_\mathrm{e} + V'_\mathrm{ei})\bigr]\bigr) \tag{10.8.10}$$

If the homogeneous electron gas is taken as the reference system, and $V'_{\rm ei}$ is again treated as a perturbation, $F'_{\rm e}$ is obtained from the coupling-parameter formula (5.2.5) as[47]

$$F'_{\rm e} = F_{\rm e} + \int_0^1 \langle V'_{\rm ei}\rangle_\lambda \, {\rm d}\lambda \tag{10.8.11}$$

where $F_{\rm e}$ is the free energy of the reference system and the subscript λ shows that the average is to be taken over an ensemble characterised by the hamiltonian $\mathcal{H}'_{\rm e} + \lambda V'_{\rm ei}$. From (10.8.5), with $\hat{v}_{\rm ei}(k)$ replaced by $\hat{v}^*_{\rm ei}(k)$, we find that for a fixed ionic configuration:

$$\langle V'_{\rm ei}\rangle_\lambda = U_0 + \frac{1}{V}{\sum_{\mathbf{k}}}' \hat{v}^*_{\rm ei}(k)\rho^{\rm i}_{\mathbf{k}}\langle\rho^{\rm e}_{-\mathbf{k}}\rangle_\lambda \tag{10.8.12}$$

The result of first-order perturbation theory corresponds to setting $\lambda = 0$. But $\langle\rho^{\rm e}_{-\mathbf{k}}\rangle_0$ is zero because the reference system is homogeneous; the second term on the right-hand side of (10.8.12) therefore disappears and we are led back to our earlier result. To obtain the second-order term it is sufficient to calculate the components of the induced electron density to first order in $\lambda V'_{\rm ei}$. If $\chi_{\rm e}(k)$ is the static electron-density response function, the induced density is

$$\langle\rho^{\rm e}_{-\mathbf{k}}\rangle_\lambda = \chi_{\rm e}(k)\lambda\hat{v}^*_{\rm ei}(k)\rho^{\rm i}_{-\mathbf{k}} \tag{10.8.13}$$

If we now substitute for $\langle V'_{\rm ei}\rangle$ in (10.8.11) and integrate over λ, we find that the free energy of the electron gas is given to second order in the electron–ion coupling by

$$F'_{\rm e} = F_{\rm e} + U_0 + \frac{1}{2V}{\sum_{\mathbf{k}}}' \chi_{\rm e}(k)\big[\hat{v}^*_{\rm ei}(k)\big]^2\rho^{\rm i}_{\mathbf{k}}\rho^{\rm i}_{-\mathbf{k}} \tag{10.8.14}$$

On comparing this result with (10.8.9) and (10.8.10) we see that the system can be regarded as a one-component fluid for which the total interaction energy is

$$V_{N_{\rm i}}\big(\{\mathbf{R}_j\}\big) = V_0 + \frac{1}{2V}{\sum_{\mathbf{k}}}' \big(\hat{v}_{\rm ii}(k) + \chi_{\rm e}(k)\big[\hat{v}^*_{\rm ei}(k)\big]^2\big)\big(\rho^{\rm i}_{\mathbf{k}}\rho^{\rm i}_{-\mathbf{k}} - N_{\rm i}\big) \tag{10.8.15}$$

where

$$V_0 = U_0 + F_{\rm e} + \tfrac{1}{2}\rho_{\rm i}{\sum_{\mathbf{k}}}' \chi_{\rm e}(k)\big[\hat{v}^*_{\rm ei}(k)\big]^2 \tag{10.8.16}$$

is independent of the structure of the liquid. Since T is normally much less than $T_{\rm F}$, $F_{\rm e}$ can be replaced by the ground-state energy of the interacting electron gas (the jellium model).

The total interaction energy may now be rewritten in a form that involves a sum of pair interactions:

$$V_{N_{\rm i}} = V_0 + \sum_{j=1}^{N_{\rm i}}\sum_{j'>j}^{N_{\rm i}} v^{\rm eff}_{\rm ii}\big(|\mathbf{R}_{j'} - \mathbf{R}_j|\big) \tag{10.8.17}$$

The effective ion–ion potential $v_{\rm ii}^{\rm eff}(R)$ is the Fourier transform of the sum of the bare ion–ion interaction $v_{\rm ii}(R)$ and an electron-induced term $v'_{\rm ii}(R)$ or, in **k**-space:

$$\hat{v}_{\rm ii}^{\rm eff}(k) = \hat{v}_{\rm ii}(k) + \hat{v}'_{\rm ii}(k) = \frac{4\pi z^2 e^2}{k^2} + \left[\hat{v}^*_{\rm ei}(k)\right]^2 \chi_{\rm e}(k)$$
$$= \frac{4\pi z^2 e^2}{k^2} + \frac{[\hat{v}^*_{\rm ei}(k)]^2}{(4\pi e^2/k^2)}\left(\frac{1}{\varepsilon_{\rm e}(k)} - 1\right) \tag{10.8.18}$$

where $\varepsilon_{\rm e}(k)$, the dielectric function of the electron gas, is related to the susceptibility $\chi_{\rm e}(k)$ in the manner of (10.2.11).[43] In the long-wavelength limit, $\varepsilon_{\rm e}(k)$ behaves as

$$\lim_{k\to 0} \varepsilon_{\rm e}(k) = 1 + k_{\rm e}^2/k^2 \tag{10.8.19}$$

with

$$k_{\rm e}^2 = k_{\rm TF}^2 \frac{\chi_{T\rm e}}{\chi_{T\rm e}^{\rm id}} \tag{10.8.20}$$

where $\chi_{T\rm e}$ and $\chi_{T\rm e}^{\rm id}$ are the isothermal compressibilities, respectively, of the interacting and non-interacting electron gas, and $k_{\rm TF} = 2(k_{\rm F}/\pi a_0)^{1/2}$ is the Thomas–Fermi wavenumber. Equation (10.8.19) is the electronic counterpart of the relation (10.2.30) satisfied by the classical OCP and $k_{\rm e}$ is the analogue of the ionic screening wavenumber $k_{\rm s}$. In the same limit, $\hat{v}^*_{\rm ei}(k) \to 4\pi z e^2/k^2$. It follows that the effective interaction $\hat{v}_{\rm ii}^{\rm eff}(k)$ is a regular function in the limit $k \to 0$, the k^{-2} singularity in the bare potential $\hat{v}_{\rm ii}(k)$ being cancelled by the same singularity in $\hat{v}'_{\rm ii}(k)$. In other words, the bare ion–ion potential $v_{\rm ii}(R)$ is completely screened by the polarisation of the electron gas, and the effective potential $v_{\rm ii}^{\rm eff}(R)$ is therefore a short-range function. A typical effective potential for an alkali metal has a soft repulsive core, an attractive well with a depth (in temperature units) of a few hundred kelvin and a weakly oscillatory tail.[48] An example of a calculated effective potential for liquid potassium is shown in Figure 1.4.

The results of the second-order calculation can be summarised by saying that we have reduced the liquid–metal problem to one of calculating the classical partition function of a fluid of $N_{\rm i}$ pseudoatoms in which the particles interact through a short-range effective potential $v_{\rm ii}^{\rm eff}(R)$. After integration over momenta, the partition function becomes

$$Q_{N_{\rm i}} = \frac{\exp(-\beta V_0)}{N_{\rm i}! \Lambda_{\rm i}^{3N_{\rm i}}} \int \exp\left(-\beta V_{N_{\rm i}}^{\rm eff}\right) {\rm d}\mathbf{R}^{N_{\rm i}} \tag{10.8.21}$$

where $V_{N_{\rm i}}^{\rm eff}$ is the sum of the pairwise-additive effective interactions for a given ionic configuration and $\Lambda_{\rm i}$ is the de Broglie thermal wavelength of the ions. Equation (10.8.21) differs from the usual partition function of a monatomic fluid in two important ways: first, in the appearance of a large, structure-independent energy V_0; and, secondly, in the fact that both V_0 and the pair potential from which $V_{N_{\rm i}}^{\rm eff}$ is derived are functions of density by virtue of the density dependence of the properties of the electron gas. The reduction of

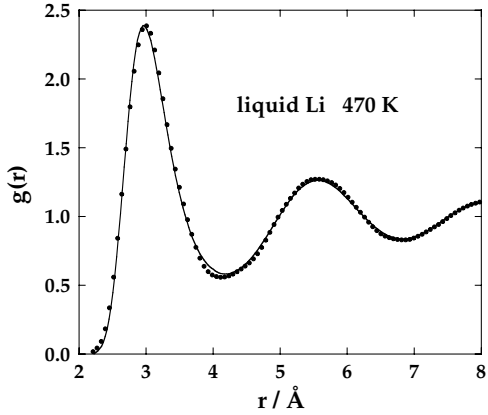

FIG. 10.9. Pair distribution function of liquid lithium near the normal melting. temperature. The curve shows results obtained by molecular-dynamics calculations for an effective ion–ion potential and the points are the results of neutron-scattering measurements. After Salmon *et al.*[50]

the problem to the form described by (10.8.21) means that the theoretical methods developed for the calculation of static properties of simple classical liquids can also be applied to liquid metals. Special care is needed only when evaluating volume derivatives of the free energy, because the density dependence of the effective interaction gives rise to extra terms. Computer simulations have shown that effective ion–ion potentials can account quantitatively for many of the observed properties of simple liquid metals. From Figure 10.9, for example, we see that the pair distribution function obtained in this way for liquid lithium[49] is in excellent agreement with that derived from neutron-diffraction data.

10.9 IONIC DYNAMICS IN LIQUID METALS

The microscopic dynamics of the ions in liquid metals do not differ in any fundamental way from the corresponding motions in simple, insulating liquids such as the rare gases. This is not surprising, since the pair potentials for metallic pseudoatoms and rare-gas atoms are qualitatively similar. For the same reason, experimental and theoretical methods that have been used successfully to study and describe the dynamics of argon-like liquids have, for the most part, met with comparable success in their application to simple liquid metals. However, as comparison of Figures 1.3 and 1.4 shows, the interactions in, say, potassium and argon do differ considerably in detail, and this gives rise to quantitative differences in the dynamical behaviour of the two types of system. For example, as we have seen in earlier chapters, experiments and simulations have combined to show that propagating collective modes of both transverse and longitudinal character persist over ranges of wavelength relative to the particle diameters that are considerably wider in liquid metals than in argon-like liquids.[51]

A different insight into the dynamics can be obtained through the representation of a liquid metal as an ion–electron plasma along the lines followed for static properties in

Section 10.8. In this picture of the liquid, the ionic and electronic components are only weakly coupled through the electron–ion pseudopotential, and each component may be regarded as an external perturbation on the other. Let $\phi_\nu(\mathbf{k},\omega)$ be an external potential that acts on component ν, where $\nu = 1$ for the ions and 2 for the electrons. Within linear-response theory the Fourier components of the induced densities are related to the external potentials by a matrix of density-response functions:

$$\left\langle \rho^\nu_{\mathbf{k}}(\omega)\right\rangle = \sum_\mu \chi_{\nu\mu}(k,\omega)\phi_\mu(\mathbf{k},\omega) \tag{10.9.1}$$

The response to the internal field is described by a similar matrix of screened response functions, $\chi^{\mathrm{sc}}_{\nu\mu}$. Written in matrix form the response is

$$\left\langle \boldsymbol{\rho}_{\mathbf{k}}(\omega)\right\rangle = \boldsymbol{\chi}^{\mathrm{sc}}(k,\omega)\cdot\left[\boldsymbol{\phi}(\mathbf{k},\omega) + \hat{\boldsymbol{v}}(k)\cdot\left\langle \boldsymbol{\rho}_{\mathbf{k}}(\omega)\right\rangle\right] \tag{10.9.2}$$

where $\hat{\boldsymbol{v}}(k)$ is the matrix of bare potentials $\hat{v}_{\nu\mu}(k)$ and the second term in square brackets is the "polarisation potential". Elimination of $\langle\rho^\nu_{\mathbf{k}}(\omega)\rangle$ between (10.9.1) and (10.9.2) leads to a matrix generalisation of the relation (10.4.11) between the external and screened response functions:

$$\boldsymbol{\chi}(k,\omega) = \boldsymbol{\chi}^{\mathrm{sc}}(k,\omega) + \boldsymbol{\chi}^{\mathrm{sc}}(k,\omega)\cdot\hat{\boldsymbol{v}}(k)\cdot\boldsymbol{\chi}(k,\omega) \tag{10.9.3}$$

or, in terms of elements of the inverse matrices:

$$\left[\boldsymbol{\chi}(k,\omega)\right]^{-1}_{\nu\mu} = \left[\boldsymbol{\chi}^{\mathrm{sc}}(k,\omega)\right]^{-1}_{\nu\mu} - \hat{v}_{\nu\mu}(k) \tag{10.9.4}$$

To lowest order in the ion–electron coupling the two species respond to the internal field as two, independent, one-component plasmas. The off-diagonal elements of $\boldsymbol{\chi}^{\mathrm{sc}}$ are then zero, and the diagonal elements $\chi^{\mathrm{sc}}_{\nu\nu}(k,\omega)$ are the screened response functions of the classical OCP ($\nu = 1$) and the degenerate electron gas in a uniform background (jellium) ($\nu = 2$). It follows, given (10.4.11) and (10.4.12), that

$$\begin{aligned}\left[\boldsymbol{\chi}^{\mathrm{sc}}(k,\omega)\right]^{-1}_{11} &= 1/\chi_{\mathrm{OCP}}(k,\omega) + \hat{v}_{11}(k)\\ \left[\boldsymbol{\chi}^{\mathrm{sc}}(k,\omega)\right]^{-1}_{22} &= \frac{\hat{v}_{22}(k)}{1-\varepsilon_{\mathrm{e}}(k,\omega)}\end{aligned} \tag{10.9.5}$$

and the external susceptibility of the ions is obtained from (10.9.4) as

$$\chi_{11}(k,\omega) = \frac{\chi_{\mathrm{OCP}}(k,\omega)}{1-\hat{v}(k,\omega)\chi_{\mathrm{OCP}}(k,\omega)} \tag{10.9.6}$$

where $\hat{v}(k,\omega)$ describes the dynamical screening of the ion–ion interaction by the electrons:

$$\hat{v}(k,\omega) = \frac{k^2[\hat{v}_{12}(k)]^2}{4\pi e^2}\left(\frac{1}{\varepsilon_{\mathrm{e}}(k,\omega)} - 1\right) \tag{10.9.7}$$

The frequency scale of the electronic motion is much higher than any frequency associated with the ions. It is therefore reasonable to make an adiabatic approximation in which $\hat{v}(k,\omega)$ is replaced by $\hat{v}(k,0)$. The characteristic frequencies of the longitudinal modes of the screened ionic plasma are given by the roots of the denominator in (10.9.6) or, in the adiabatic approximation, by the solution to the equation

$$1 - \hat{v}(k,0)\chi_{\mathrm{OCP}}(k,\omega) = 0 \tag{10.9.8}$$

In the limit $k \to 0$, the ratio $\widetilde{F}_{\mathrm{OCP}}(k,\omega)/S_{\mathrm{OCP}}(k)$ is related to the frequency-dependent electrical conductivity by (10.4.30). Thus, from (7.6.21):[52]

$$\begin{aligned}\lim_{k\to 0}\chi_{\mathrm{OCP}}(k,\omega) &= -\beta\rho_{\mathrm{i}}\lim_{k\to 0}\lim_{\varepsilon\to 0}\left[S_{\mathrm{OCP}}(k) + i(\omega+i\varepsilon)\widetilde{F}_{\mathrm{OCP}}(k,\omega+i\varepsilon)\right] \\ &= -\beta\rho_{\mathrm{i}}\lim_{k\to 0}S_{\mathrm{OCP}}(k)\lim_{\varepsilon\to 0}\frac{4\pi\sigma(\omega+i\varepsilon)}{-i(\omega+i\varepsilon)+4\pi\sigma(\omega+i\varepsilon)}\end{aligned} \tag{10.9.9}$$

The long-wavelength limit of $S_{\mathrm{OCP}}(k)$ is given by (10.2.31) and the complex conductivity $\sigma(\omega+i\varepsilon)$ can be expressed, via (7.7.10), in the form

$$\sigma(\omega+i\varepsilon) = \frac{\beta}{V}\int_0^\infty J(t)\exp\left[i(\omega+i\varepsilon)t\right]\mathrm{d}t \tag{10.9.10}$$

where $J(t)$ is the charge–current autocorrelation function. In the OCP the proportionality of mass and charge means that the conservation of total linear momentum is equivalent to the conservation of charge current, i.e. the resistivity is zero. Hence

$$J(t) = J(0) = \frac{N_{\mathrm{i}}z^2e^2k_{\mathrm{B}}T}{m_{\mathrm{i}}} \tag{10.9.11}$$

and, from (10.9.10):

$$\sigma(\omega+i\varepsilon) = \frac{i\omega_{\mathrm{pi}}^2}{4\pi(\omega+i\varepsilon)} \tag{10.9.12}$$

where $\omega_{\mathrm{pi}}^2 = 4\pi\rho_{\mathrm{i}}z^2e^2/m_{\mathrm{i}}$ is the square of the ionic plasma frequency. Substitution of (10.9.12) in (10.9.9) shows that

$$\lim_{k\to 0}\frac{\chi_{\mathrm{OCP}}(k,\omega)}{S_{\mathrm{OCP}}(k)} = \frac{\beta\rho_{\mathrm{i}}\omega_{\mathrm{pi}}^2}{\omega^2-\omega_{\mathrm{pi}}^2} \tag{10.9.13}$$

At small k, $\varepsilon_{\mathrm{e}}(k,0) \approx k_{\mathrm{e}}^2/k^2$, from (10.8.19), and $\hat{v}_{12}(k)$, in the empty-core model, behaves as

$$\hat{v}_{12}(k) = \frac{4\pi z^2e^2\cos kr_{\mathrm{c}}}{k^2} \approx \frac{4\pi ze^2}{k^2}\left(1-\tfrac{1}{2}k^2r_{\mathrm{c}}^2\right) \tag{10.9.14}$$

so that

$$\lim_{k\to 0}\hat{v}(k,0)=\frac{4\pi z^2e^2}{k^2}\left(1-k^2r_c^2\right)\left(\frac{k^2}{k_e^2}-1\right) \tag{10.9.15}$$

When the results are brought together we find that to order k^2 the solution to (10.9.8) leads to a dispersion relation characteristic of a propagating sound wave, i.e.

$$\omega=\omega_{pi}\left(k_e^{-2}+k_s^{-2}+r_c^2\right)^{1/2}k=ck \tag{10.9.16}$$

where k_s is the ionic screening wavenumber defined by (10.2.28) and c is the speed of sound. Thus the effect of electron screening is to convert the plasmon mode at frequency ω_{pi} into a sound wave of a frequency that vanishes linearly with k. A more detailed analysis shows that c can be identified with the isothermal speed of sound, but this differs little from the adiabatic value, since the ratio of specific heats is close to unity for liquid metals.

NOTES AND REFERENCES

1. Gillan, M.J., *In* "Ionic Solids at High Temperatures" (A.M. Stoneham, ed.). World Scientific, Singapore, 1989.
2. For a review of the properties of the OCP, see Baus, M. and Hansen, J.P., *Phys. Rep.* **59**, 1 (1980).
3. Tosi, M.P. and Fumi, F.G., *J. Phys. Chem. Solids* **25**, 45 (1964).
4. Wilson, M. and Madden, P.A., *J. Phys. Condens. Matter* **5**, 2687 (1993).
5. Sprik, M. and Klein, M.L., *J. Chem. Phys.* **89**, 7558 (1988).
6. Martin, P.A. and Yalcin, T., *J. Stat. Phys.* **31**, 691 (1983).
7. (a) Stillinger, F.H. and Lovett, R., *J. Chem. Phys.* **48**, 3858 (1968). (b) Stillinger, F.H. and Lovett, R., *J. Chem. Phys.* **49**, 1991 (1968).
8. Blum, L., Gruber, C., Lebowitz, J.L. and Martin, P.A., *Phys. Rev. Lett.* **48**, 1769 (1982).
9. Giaquinta, P.V., Parrinello, M. and Tosi, M.P., *Phys. Chem. Liq.* **5**, 305 (1976).
10. Hansen, J.P. and McDonald, I.R., *Phys. Rev. A* **11**, 2111 (1975).
11. Waisman, E. and Lebowitz, J.L., *J. Chem. Phys.* **56**, 3086 and 3091 (1972).
12. Rasaiah, J.C., Card, D.N. and Valleau, J.P., *J. Chem. Phys.* **56**, 248 (1972).
13. Larsen, B., *J. Chem. Phys.* **65**, 3431 (1976).
14. (a) Høye, J.S., Stell, G. and Waisman, E., *Mol. Phys.* **32**, 209 (1976). (b) Høye, J.S. and Stell, G., *J. Chem. Phys.* **67**, 524 (1977).
15. Valleau, J.P., Cohen, L.K. and Card, D.N., *J. Chem. Phys.* **5942** (1980).
16. See, e.g., Duh, D.-M. and Haymet, A.J., *J. Chem. Phys.* **97**, 7716 (1992).
17. Bresme, F., Lomba, E., Weis, J.J. and Abascal, J.L.F., *Phys. Rev. E* **51**, 289 (1995).
18. See the discussion surrounding (4.7.2).
19. Ballone, P., Pastore, G. and Tosi, M.P., *J. Chem. Phys.* **81**, 3174 (1984).
20. Zerah, G. and Hansen, J.P., *J. Chem. Phys.* **84**, 2336 (1986).
21. Abramo, M.C., Parrinello, M. and Tosi, M.P., *J. Non-Metals* **2**, 67 (1973).
22. Cohen, C., Sutherland, J.W.H. and Deutch, J.M., *Phys. Chem. Liq.* **2**, 213 (1971).
23. (a) Sjögren, L. and Yoshida, F., *J. Chem. Phys.* **77**, 3703 (1982). (b) Munakata, T. and Bosse, J., *Phys. Rev. A* **27**, 455 (1983).
24. See, e.g., Morgan, B. and Madden, P.A., *J. Chem. Phys.* **120**, 1402 (2004).
25. See, e.g., Madden, P.A. and O'Sullivan, K.F., *J. Chem. Phys.* **95**, 1980 (1991).
26. Bosse, J. and Munakata, T., *Phys. Rev. A* **25**, 2763 (1982).
27. Giaquinta, P.V., Parrinello, M. and Tosi, M.P., *Physica A* **92**, 185 (1978). The Raman spectra of molten salts can also be analysed in terms of fluctuations in mass and charge densities: see ref. 24.

28. Jackson, J.D., “Classical Electrodynamics”, 3rd edn. John Wiley, New York, 1999.
29. Stillinger, F.H., *J. Chem. Phys.* **35**, 1584 (1961). See also Allen, R.J., Hansen, J.P. and Melchionna, S., *Phys. Chem. Chem. Phys.* **3**, 4177 (2001).
30. This definition is already implicit in (10.2.6).
31. Henderson, D. and Blum, L., *J. Chem. Phys.* **69**, 5441 (1978).
32. For a review of approximations beyond Poisson–Boltzmann theory, see Hansen, J.P. and Löwen, H., *Ann. Rev. Phys. Chem.* **51**, 209 (2000).
33. (a) Guldbrand, L., Jönsson, B., Wennerström, H. and Linse, P., *J. Chem. Phys.* **80**, 2221 (1984). (b) Valleau, J.P., Ivkov, R. and Torrie, G.M., *J. Chem. Phys.* **95**, 520 (1991).
34. Tang, Z., Scriven, L.E. and Davis, H.T., *J. Chem. Phys.* **97**, 9258 (1992).
35. (a) Kjellander, R., Åkesson, T., Jönsson, B. and Marčelia, S., *J. Chem. Phys.* **97**, 1424 (1992). (b) Greberg, H. and Kjellander, R., *J. Chem. Phys.* **108**, 2940 (1998).
36. Löwen, H., Hansen, J.P. and Madden, P.A., *J. Chem. Phys.* **98**, 3275 (1993).
37. Car, R. and Parrinello, M., *Phys. Rev. Lett.* **55**, 247 (1985).
38. We ignore any non-coulombic component of the external potential.
39. Verwey, E.J.W. and Overbeek, J.T.G., “Theory of Stability of Lyophobic Colloids”. Elsevier, Amsterdam, 1948.
40. (a) van Roij, R., Dijkstra, M. and Hansen, J.P., *Phys. Rev. E* **59**, 2010 (1999). (b) van Roij, R. and Evans, R., *J. Phys. Condens. Matter* **11**, 1004 (1999).
41. (a) Belloni, L., *Colloids Surf. A* **140**, 227 (1998). (b) Bocquet, L., Trizac, E. and Aubouy, M., *J. Chem. Phys.* **117**, 8138 (2002).
42. Crocker, J.C. and Grier, D.G., *Phys. Rev. Lett.* **73**, 352 (1994).
43. Pines, D. and Nozières, P., “The Theory of Quantum Liquids”. W.A. Benjamin, New York, 1966.
44. Ashcroft, N.W. and Stroud, D., *Sol. State Phys.* **33**, 1 (1978).
45. Ashcroft, N.W., *J. Phys. C* **1**, 232 (1966).
46. (a) Hansen, J.P., *Phys. Rev. A* **8**, 3096 (1973). (b) Slattery, W.L., Doolen, G.D. and DeWitt, H.E., *Phys. Rev. A* **21**, 2087 (1980).
47. Note that the prime has different meanings in (5.2.5) and (10.8.11).
48. The oscillatory behaviour at large separations is linked to a logarithmic singularity in the dielectric function. See Faber, T.E., “An Introduction to the Theory of Liquid Metals”. Cambridge University Press, Cambridge, 1972, p. 28.
49. The potential used in the simulations was derived from an empty-core pseudo-potential with a core radius obtained by fitting to the height of the first peak in the experimental structure factor: Anento, N., Canales, M. and Gonzàlez, L.E., unpublished results. See also Canales, M., Gonzàlez, L.E. and Pàdro, J.A., *Phys Rev. E* **50**, 3656 (1994).
50. Salmon, P.S., Petri, I., de Jong, P.H.K., Verkerk, P., Fischer, H.E. and Howells, W.S., *J. Phys. Condens. Matter* **16**, 195 (2004).
51. For a review of experimental results on liquid metals, see Scopigno, T., Ruocco, G. and Sette, F., *Rev. Mod. Phys.* **77**, 881 (2005).
52. The origin of the minus sign in (10.9.9) is explained in Section 7.6.